



# Catalog of the Galactic Population of X-Ray Pulsars in High-mass X-Ray Binary Systems

Vitaliy Kim , Ildana Izmailova , and Yerlan Aimuratov

Fesenkov Astrophysical Institute, Observatory 23, 050020, Almaty, Kazakhstan; [kim@fai.kz](mailto:kim@fai.kz), [ursamajoris1987@gmail.com](mailto:ursamajoris1987@gmail.com)

Received 2022 September 21; revised 2023 June 29; accepted 2023 July 10; published 2023 September 4

## Abstract

A catalog of the Galactic population of X-ray pulsars in high-mass X-ray binary (HMXB) systems is presented. It contains information about 82 confirmed sources: 18 persistent and 64 transient pulsars. Their basic parameters include spin period, spin evolution with global and local spin-up/spin-down and duration, orbital period, X-ray luminosity, magnetic field strength measured by cyclotron line analysis, distance, spectral and luminosity class, and observable parameters of massive companions, which are shown in the tables provided, with corresponding references. Candidates of HMXB pulsars are also listed for further careful consideration.

*Unified Astronomy Thesaurus concepts:* High mass x-ray binary stars (733); Neutron stars (1108); Pulsars (1306); Accretion (14); High energy astrophysics (739)

*Supporting material:* machine-readable tables

## 1. Introduction

High-mass X-ray binaries (HMXBs) are systems consisting of two components: the first is a massive star of the early spectral class, and the second can be presented as a degenerated object—a neutron star (NS), black hole, or white dwarf (in rare cases). A significant difference from other massive binaries is the presence of X-ray emission in these systems for most cases, due to accretion (Liu et al. 2006; Fortin et al. 2023; Neumann et al. 2023). Observable parameters and characteristics of HMXBs give important information for modeling and understanding binary systems’ accretion and stellar evolution processes. One of the largest HMXB subclasses is X-ray pulsars.

HMXB X-ray pulsars are close pairs of stars, one of which is an NS, and its companion is a massive star of early (O–B or Be) spectral type. The massive components of these systems usually do not fill their Roche lobe, but experience a significant loss of matter in the form of a stellar wind with a rate of  $10^{-6}$ – $10^{-7} M_{\odot} \text{ yr}^{-1}$  (Liu et al. 2006). As the NS orbits its companion, it picks up some of the matter from stellar wind and accretes it onto its surface. This mechanism of mass exchange is called accretion from the stellar wind or wind accretion (Davidson & Ostriker 1973). The fundamental difference between HMXB X-ray pulsars and most other types of X-ray pulsars is that the mass exchange between the components of these systems occurs in the wind accretion mode.

Periodic changes in the X-ray intensity of these pulsars are usually associated with their spin rotation, which modulates the pulsations, and with a sufficiently strong magnetic field, which affects the nature of the motion of the matter near the NS and leads to an inhomogeneous temperature distribution of its surface (Lyne & Graham-Smith 2012).

Until recently, the most complete catalog of HMXBs was published more than 15 yr ago and, to that date, collected information about 64 X-ray pulsars in binary systems (Liu et al.

2006). Since then, new sources have been discovered, a few candidates were confirmed to be not pulsars, and information about already known sources was clarified and supplemented. Recently, HMXB catalogs have been released by Fortin et al. (2023) and independently by Neumann et al. (2023), with updated information about the Galactic population of HMXBs. Additionally, the progress in spaceborne missions has resulted in various all-sky surveys, some of them focusing on the hard X-ray domain (Krivonos et al. 2022), which can also be used for an extensive search for pulsars in HMXBs. All of these catalogs give general information about HMXBs without focusing on X-ray pulsars.

We conducted our independent crossmatching analysis of existing catalogs and databases, such as the Fortin (including Liu), Neumann, and Krivonos catalogs, as well as the Compton Gamma Ray Observatory (CGRO), Fermi, and SIMBAD databases, to search for X-ray pulsars identified with NSs in massive binary systems. Based on the analysis results, we have created a complete catalog (as of 2023 April) of the Galactic population of X-ray pulsars in HMXB systems containing data from 82 sources.

In contrast to the general HMXB catalogs, we have concentrated our efforts on finding and providing detailed information about the parameters of pulsars, such as spin and orbital periods, data on the evolution of pulsar spin periods, X-ray luminosity of the source, and magnetic fields measured from cyclotron lines. Moreover, the catalog contains, where available, detailed information about the parameters of the massive companions: proper name or identification number, spectral type, luminosity class, photometric estimates of the brightness of the companion in the optical and infrared regions, color excess, as well as information about the coordinates of the objects and estimates of their distance.

For the sake of convenience, we split the catalog into two parts as persistent (Table 2 in the Appendix) and transient (Table 3 in the Appendix) pulsars in HMXBs. We provide discussions of notable confirmed HMXB pulsars and separately of candidates, highlighting the extreme or peculiar properties found during their observations. We attempt to provide comprehensive literature on the cataloged sources, although we do not claim to be complete.



Original content from this work may be used under the terms of the [Creative Commons Attribution 4.0 licence](#). Any further distribution of this work must maintain attribution to the author(s) and the title of the work, journal citation and DOI.

The catalog can be useful for studying stellar evolution in binary systems in late stages (Chaty 2022), for studying the distribution of the NS population in the Galaxy (Coleiro & Chaty 2013), for studying and modeling a stellar wind and its parameters from hot stars (de Burgos et al. 2023), and for studying the massive components in HMXBs (Kretschmar et al. 2017), by analyzing the generated X-ray flux from the NS and its spin evolution, etc.

## 2. Building the Catalog

We base our searches on catalogs and data from various space missions of the last decades as well as on an extensive review of the literature via the SAO/NASA Astrophysics Data System (ADS)<sup>1</sup> and SIMBAD astronomical database (Wenger et al. 2000). A coordinate crossmatching method of three catalogs was used to collect the core of our HMXB pulsars catalog. As a basic criterion, we took an NS to be the main X-ray active component of the binary, thus excluding black hole HMXBs from our consideration. A reduced sample has been searched for additional data to collect only confirmed HMXB pulsars, therefore we excluded candidates, erroneous identifications, and misclassifications. To complete the catalog, we gathered information on massive companions, focusing on the main information, including spectral type, luminosity, and photometric brightness. Finally, we separately collected information on candidates of HMXB pulsars from elsewhere, for ease of further investigations.

### 2.1. Reference Catalogs

There are recently published catalogs on Galactic HMXBs. They came to update a commonly referenced work—the Fourth HMXB Catalog by Liu et al. (2006), which in turn was the last in a sequence of works (Bradt & McClintock 1983; van Paradijs 1995; Liu et al. 2000) dedicated to systematically collecting information on HMXBs.

Fortin et al. (2023) provide a catalog of 152 HMXBs in the Galaxy collected up to the end of 2022. Based on a catalog by Liu et al. (2006), they formed a working sample via crossmatching with a catalog of hard X-ray sources by Bird et al. (2016). A data set has been further complemented by querying HMXBs from the SIMBAD database and enhanced by positional crossmatching with available counterparts from various space missions.

The catalog by Neumann et al. (2023) presents information and characteristic properties of 169 HMXBs in the Galaxy collected by 2022 October. The authors have also used Liu's catalog and cross-correlated it with INTEGRAL and Neil Gehrels Swift Observatory data sets obtained between 2002 and 2020 (Kretschmar et al. 2019). The catalog was enhanced by a systematic search of the literature and querying HMXBs from the SIMBAD and VizieR databases.

The above catalogs aimed to provide updated basic information on Galactic HMXBs. Both have used the catalog by Liu et al. (2006) as a core and cross-correlated it with databases of space missions of different years. Fortin et al. (2023) used the INTEGRAL observations summarized in Bird et al. (2016), where the data were collected between 2002 and 2010. Neumann et al. (2023) used INTEGRAL data summarized in Kretschmar et al. (2019). We aim to further utilize these

**Table 1**  
Crossmatch of Three Catalogs and Resulting HMXB Pulsar Catalog

Catalog	Krivonos et al. (2022)	Fortin et al. (2023)	Neumann et al. (2023)
Krivonos et al. (2022)	929	100	101
Fortin et al. (2023)	100	152	147
Neumann et al. (2023)	101	147	169
82 HMXB pulsars (this work)	65	79	81

reference catalogs and form a list of X-ray pulsars in HMXBs. To eliminate the discrepancies between Fortin's and Neumann's lists, since each of them used slightly different sources and methods for sampling, we support our coordinate crossmatch by including recently obtained all-sky survey data observed in hard X-ray within 17 yr by the INTEGRAL/IBIS detector (Krivonos et al. 2022). Pulsar lists by the Fermi Gamma-Ray Burst Monitor (GBM; Fermi Collaboration 2022) and CGRO-BATSE (CGRO Collaboration 2000) were also used to extract information on the collected objects. We gathered literature and extensively used the SIMBAD database to complete our catalog with the most comprehensive information on pulsars in HMXBs.

### 2.2. Data Collection and Selection Methods

We conducted a coordinate crossmatch method for three catalogs: Krivonos et al. (2022), Fortin et al. (2023), and Neumann et al. (2023)—cumulatively they contain 1000 objects of various types. To search for the catalog data, the capabilities of the Virtual Observatory were used via TOPCAT (Taylor 2005). The data were retrieved via the Table Access Protocol (TAP) query using the following algorithm. The keyword for finding a service containing the Fortin et al. (2023) catalog was `fortin`, which corresponded to TapVizier service.<sup>2</sup> In the service, the request was made via `Description` and the `fortin` keyword. The required table was found through a manual search of the table descriptions. The keyword was necessary because when using the service, the user gets access to all data and tables, so a set of results correspond to a given query. In the future, for a faster search, the table name of the tab `J/A+A/665/A31/table1` could be used in TapVizier. The catalog by Krivonos et al. (2022) was retrieved from the website.<sup>3</sup> The catalog data in Neumann et al. (2023) were retrieved from the catalog website.<sup>4</sup>

For the coordinate crossmatch of each pair of the three catalogs in TOPCAT, a search radius of 10' was used, since it is the maximal radius used in these catalogs that corresponds to the accuracy of the positioning of the objects by the INTEGRAL observatory. In addition, Match Selection with “Best match, symmetrical” and Join Type with the criteria “1 and 2” were used as Output Rows parameters. A pairwise comparison of the tables resulted, with the objects contained in each pair of the directories (Table 1). Further matching of any of the resulted pairs with the third

<sup>2</sup> <http://tapvizier.cds.unistra.fr/TAPVizier/tap>

<sup>3</sup> <https://integral.cosmos.ru>

<sup>4</sup> <http://astro.uni-tuebingen.de/~xrbcat/HMXBcat.html>

<sup>1</sup> <https://ui.adsabs.harvard.edu>

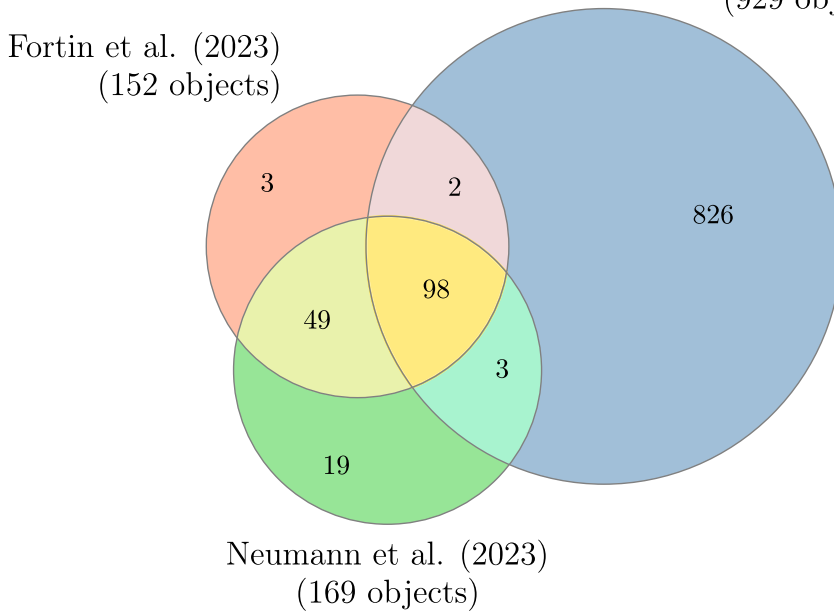


**Figure 1.** Venn diagram of the coordinate crossmatch of the three catalogs (not to scale). Each colored sector indicates the number of unique objects present either in the single catalog (3, 19, and 826), in two catalogs (2, 3, and 49), or in all three catalogs (98).

catalog gives a list of objects contained in all of the three directories.

A Venn diagram in Figure 1 schematically illustrates the crossmatching process. Each sector indicates the number of unique objects present either in the single catalog (3, 19, and 826, colored respectively in coral, light green, and steel blue) or in two catalogs (2, 3, and 49, colored respectively in light pink, cyan, and olive), or in all three catalogs (98, colored in gold), the latter being the working core of the catalog under construction. This golden sector and the remaining supplementary sectors are further investigated individually by applying selection criteria.

From Neumann's and Fortin's data, we select sources that have regular pulsations in their X-ray emission, i.e., having the `P_PULSE` parameter. However, not all objects with `P_PULSE` are X-ray pulsars. We apply a criterion to exclude black holes, nonmagnetized (or weakly magnetized) NSs, and unidentified objects as active X-ray components. Among the remaining objects, we have X-ray pulsars (confirmed and candidates), pulsating white dwarfs, and objects with pulsations caused by other processes, i.e., not associated with spin rotation. In the resulting list, we examine each object in the SAO/NASA ADS and SIMBAD databases, thereby selecting the sources confirmed as X-ray pulsars.

Another sampling criterion should be applied to Krivonos' data set from the INTEGRAL all-sky survey, which was obtained mainly in the hard X-ray and gamma-ray ranges. First of all, we select only Galactic objects (Category = Galactic), and then we apply an additional selection for which the Type parameter meets the criterion of HMXBs (Type = HMXB).

The selection by the `P_PULSE` parameter reduced the working core (golden sector) by 35 discarded objects. The remaining 63 sources in the golden core were complemented with 18 confirmed HMXB pulsars found in either Fortin's or Neumann's lists and one object found in Krivonos' list. In the supplementary sectors, we were able to find that three objects

(Swift J1845.70037, IGR J18179-1621, and IGR J17200-3116) identified as X-ray pulsars are missing from Fortin's catalog, one object (Swift J1845.70037) is missing from Neumann's catalog, and 17 objects (SAX J0635.2+0533, XTE J1829-098, IGR J18179-1621, Swift J1626.6-5156, XTE J1543-568, RX J0 812.4-3114, 1H 2138+579, XTE J1906+09, 1H 1238-599, GRO J2058+42, SGR 0755-2933, IGR J21343+4738, IGR 06 074+2205, MAXI J1409-619, SAX J2239.3+6116, SAX J1 324.4-6200, and AX J1910.7+0917) are missing from Krivonos' catalog (see the last row in Table 1). Thus, the complete catalog of confirmed pulsars in HMXB contains 82 sources.

### 3. Catalog Objects

#### 3.1. HMXB Pulsars and Their Classification: Persistent Sources and Transients

X-ray pulsars in massive binary systems are relatively numerous compared to other types of X-ray pulsars. The current population of Galactic HMXB pulsars includes 82 objects, and all of them (except X Per) have absolute values of galactic latitude not exceeding  $4.1^\circ$  (see Figure 2). Most of them are located within  $\sim 2\text{--}10$  kpc from the galactic plane (Coleiro & Chaty 2013).

X-ray pulsars in HMXBs are usually divided into two main groups: persistent sources and transients. Persistent pulsars constitute a group of sources where the X-ray flux experiences only smooth variations without outburst activity over the entire period of observations (Reig & Roche 1999); see the left column in Figure 3. This implies a relatively stable outflow of matter from their massive companions, with a stable accretion rate on the NS surface (Reig & Roche 1999).

The galactic population of persistent pulsars includes 18 sources, the luminosity of which lies in the range  $10^{34}\text{--}10^{37}$  erg s $^{-1}$ . They have been observed in systems with relatively short orbital periods, for most cases  $<20$  days, and small orbital eccentricity (Tutukov & Cherepashchuk 2020).

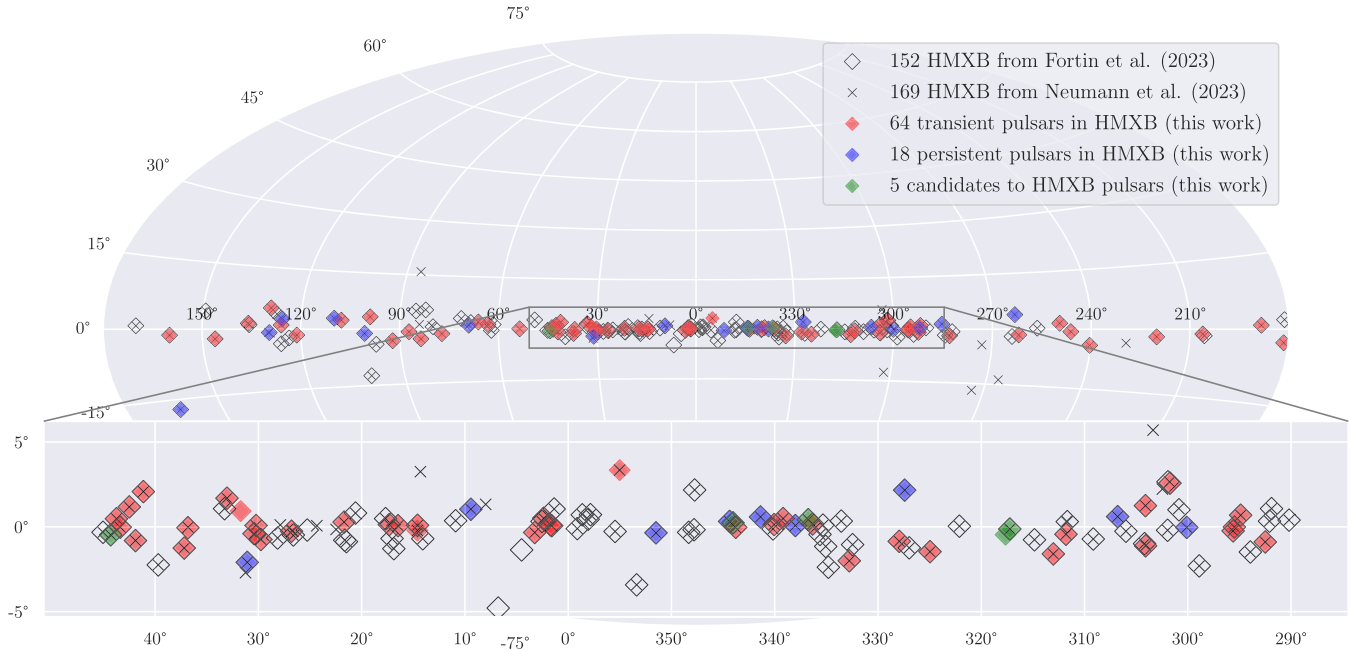


**Figure 2.** Distribution of the Galactic HMXB sources in Aitoff projection. The inset resolves the dense central region. Crosses indicate objects from the catalog by Neumann et al. (2023), while empty diamonds show the objects from the catalog by Fortin et al. (2023). Transient (red) and persistent (blue) pulsars in HMXBs are indicated by the coloring of the corresponding crosses, diamonds, or both. Crosses and diamonds without coloring indicate HMXBs with a black hole as the main X-ray active component. Candidates of pulsars are colored green. All HMXB X-ray pulsars (except X Per) have absolute values of galactic latitude not exceeding 4°1.

Exceptions, however, are X Per, with an orbital period of  $P_{\text{orb}} \sim 250$  days (Delgado-Martí et al. 2001) and RX J0146.9 +6121, with  $P_{\text{orb}} \sim 330$  days (Sarty et al. 2009). Most of the persistent X-ray pulsars are long-periodic, with  $P_s > 100$  s and reaching 9475 s. Exceptions are Cen X-3, OAO 1657, and IGR J22534+6243; their spin periods are less than 100 s.

The galactic population of transient pulsars currently includes 64 objects. On the contrary, they are characterized by rapid changes in the magnitude of the X-ray flux by several orders of magnitude; see the right column in Figure 3. Transients, compared to persistent pulsars, have larger orbital periods and larger orbital eccentricity  $\varepsilon > 0.2$  (Tutukov & Cherepashchuk 2020; Fortin et al. 2023), reaching  $\varepsilon \simeq 0.88$  in GS 1843-02 (Finger et al. 1999).

The X-ray luminosities of persistent sources and the majority of transient pulsars in a quiescent state are found within  $10^{34}$ – $10^{37}$  erg s $^{-1}$ . According to Negueruela (1998), the outbursts of transient pulsars, in most cases, can be classified as follows:

1. Short X-ray outbursts (or first-type outbursts) are characterized by a rapid increase in luminosity by an order of magnitude and have durations of several days. For some sources, they occur near the periastron and have a periodicity comparable to the orbital period;
2. Giant X-ray outbursts (or second-type outbursts) are characterized by a significant increase in X-ray luminosity, up to several orders of magnitude and several weeks in duration. This type of outburst, in most cases, does not correlate with the orbital period.

The spectra of X-ray pulsars within 1–10 keV are predominantly of a blackbody origin. An exponential cutoff is generally observed in the hard part of the spectrum. However, power-law “tails” are observed occasionally (Lipunov 1992; Coburn et al. 2002).

### 3.2. Pulsar Spin and Its Evolution

The spin periods ( $P_s$ ) of X-ray pulsars in HMXBs are dispersed over a wide range of values. The periods of most pulsars whose radiation is generated during the accretion process are within the range from 2.76 to 36,200 s. The exceptions are the first object in Table 3 in the Appendix (SAX J0635.2+0533), the transient pulsar whose period is less than a second. There is, however, a reason to believe that the radiation from these objects is not of an accretionary nature (see Section 4).

It should be especially noted that the spin periods of pulsars are not constant and change over time (see Figure 4), undergoing:

1. Global trends of spin-up (or spin-down) taking place with rates usually  $|\dot{\nu}| < 10^{-12}$  Hz s $^{-1}$ , where  $\dot{\nu} = d\nu/dt$  and  $\nu = 1/P_s$  is the spin frequency of a pulsar. These trends usually can last from several months to several years and, in some cases, up to decades.
2. Episodic variations (local trends) of spin-up (or spin-down). These chaotic variations occur at an exceptionally high rate. They can be an order of magnitude or more superior to global trends and last from several days to several weeks. Episodic variations take place against the backdrop of global trends.

Even in the first decades after the discovery of X-ray pulsars, it was noted that the vast majority of such objects experience a peculiar global spin-up (Lipunov 1992). There are several hypotheses about the origin of this phenomenon:

1. Siuniaev & Shakura (1977) proposed a hypothesis that during the evolution of the massive component of the system, the intensity of the outflow of its stellar wind can increase, which leads to the global spin-up of an NS in the system. However, this hypothesis raises serious

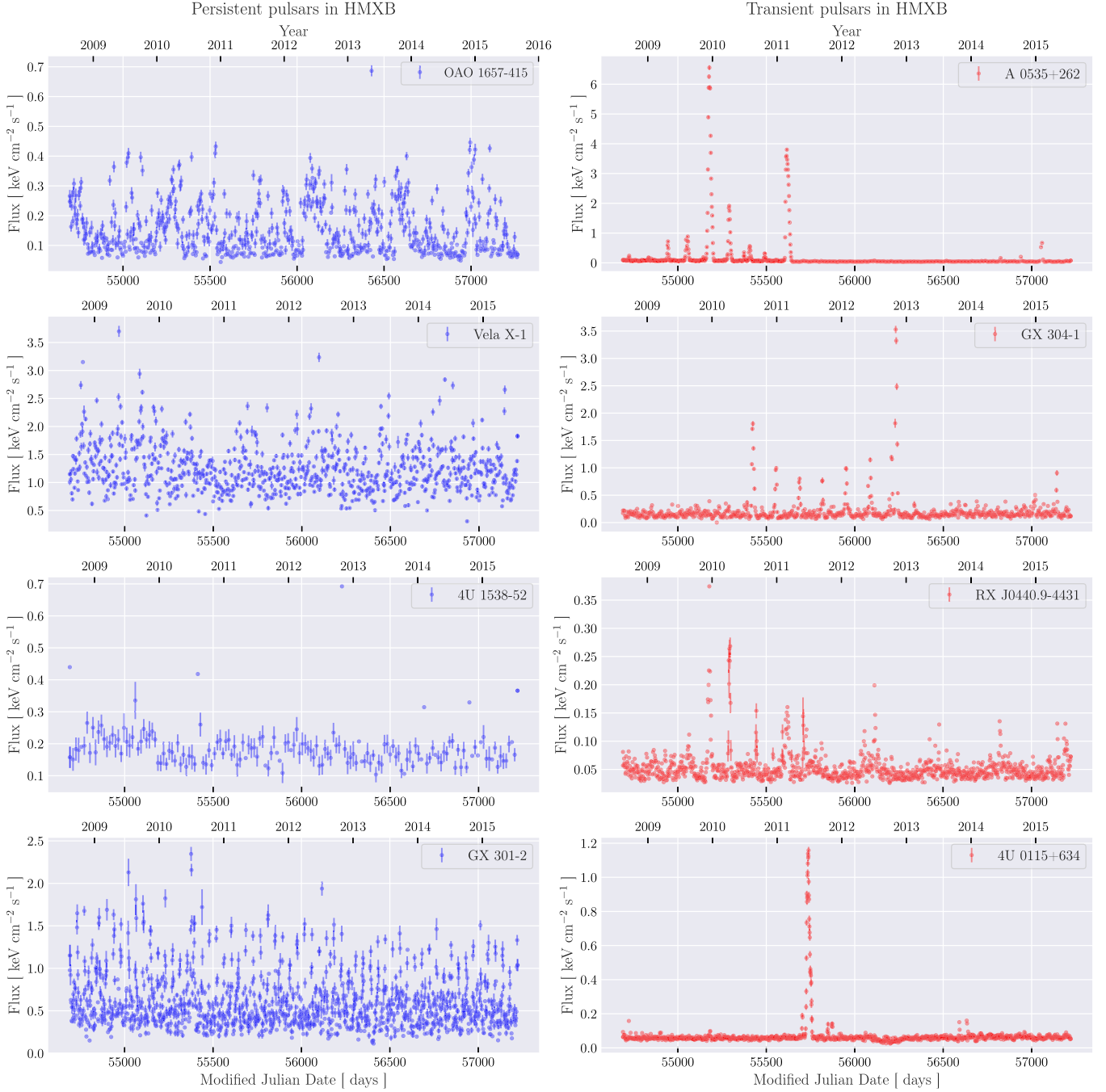


**Figure 3.** Observed flux (in  $\text{keV cm}^{-2} \text{s}^{-1}$ ) for a time in Modified Julian Date (MJD) by Fermi-GBM (Fermi Collaboration 2022) from some persistent (left column) and transient (right column) X-ray pulsars in the range 12–50 keV.

doubts (Lipunov 1992), since the evolution of stars is insignificant on a scale of several decades.

2. Selection effects. According to this hypothesis, pulsar acceleration occurs at the accretion stage (Ghosh & Lamb 1979a, 1979b). The deceleration occurs when an NS does not manifest as a variable X-ray source at the propeller stage. This hypothesis also raises doubts, since accreting X-ray pulsars rotate near the equilibrium period, which can be much larger than the critical period for the transition to the propeller stage.
3. The durations of the stages of spin-up and spin-down of the pulsar are asymmetric. The spin-up phase has a longer and gentler trend, while the spin-down phase occurs over a

short time, but at a faster rate. Therefore, the probability of observing a pulsar in the spin-up stage is higher. Such a scenario can occur when the scalar potential is asymmetric on the side of the accretion flow (Lipunov 1992).

4. Kim & Ikhsanov (2017) proposed a hypothesis about long-period variations in the stellar wind of massive companions using the pulsar OAO 1657-415 as an example. Local variations of the spin-up/spin-down of pulsars are approximately an order of magnitude higher than the value of its global acceleration trend, which speaks in favor of the equilibrium rotation of the pulsar, i.e., the spin rotation of an NS with an equilibrium period. The torque carried by the accretion flow to the NS

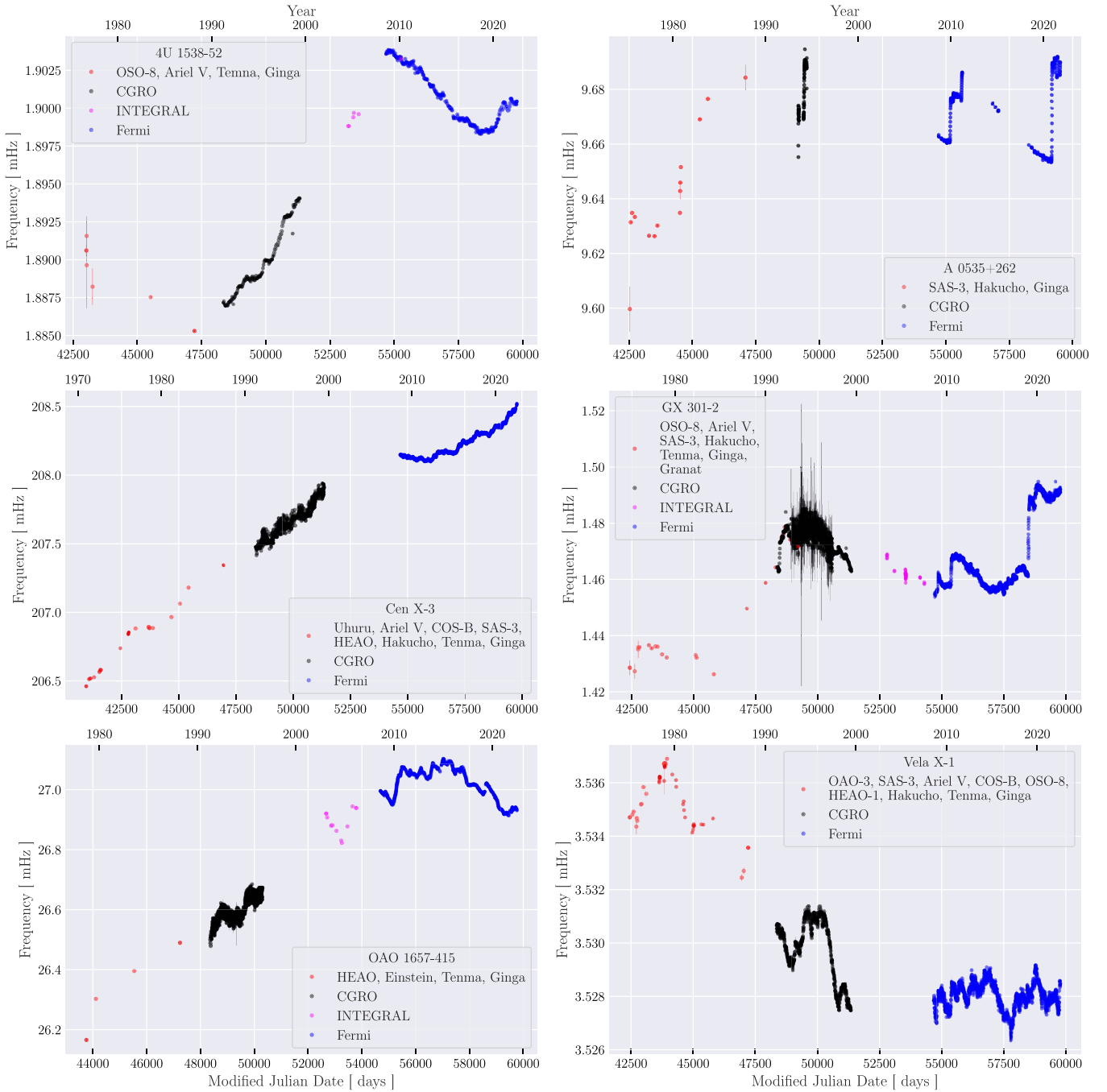


**Figure 4.** Evolution of the spin period (frequency) of some Galactic X-ray pulsars in HMXBs within the time range from the 1970s to 2022 received by HEAO-1, Tenma, Ginga, Einstein, OSO-8, Ariel V, and Granat (red; Nagase 1989), the CGRO (black; CGRO Collaboration 2000), INTEGRAL (magenta; Integral Collaboration 2022), and Fermi-GBM (blue; Fermi Collaboration 2022). The error bars for later missions are within data points due to the increase in instrumental precision.

essentially depends on the velocity of the stellar wind. The observed global trends in spin-up and spin-down may be due to the drift of the equilibrium period caused by apparently long-term changes in the wind velocity of massive components in HMXBs. Similar long-term velocity variations are also observed in the solar wind associated with the 11 yr activity cycle (Li et al. 2017).

In most cases, the observed changes in the spin periods of X-ray pulsars in HMXBs are associated with the angular momentum exchange between the NS and its accretion flow. In

this case, the efficiency of the angular momentum exchange depends on the parameters of the HMXB system and the realized accretion scenario: quasi-spherical (QSp) accretion (Davidson & Ostriker 1973; Arons & Lea 1976), Keplerian disk (Kd; Pringle & Rees 1972; Shakura 1973), MAD-disk (or ML-disk; Ikhshanov et al. 2014), etc.

In Figure 5, we show the  $P_s - |\dot{P}|$  diagram for Galactic X-ray pulsars in HMXBs with known spin evolution. As mentioned above, these observable processes are due to angular momentum exchange. In such a case, the torque applied to

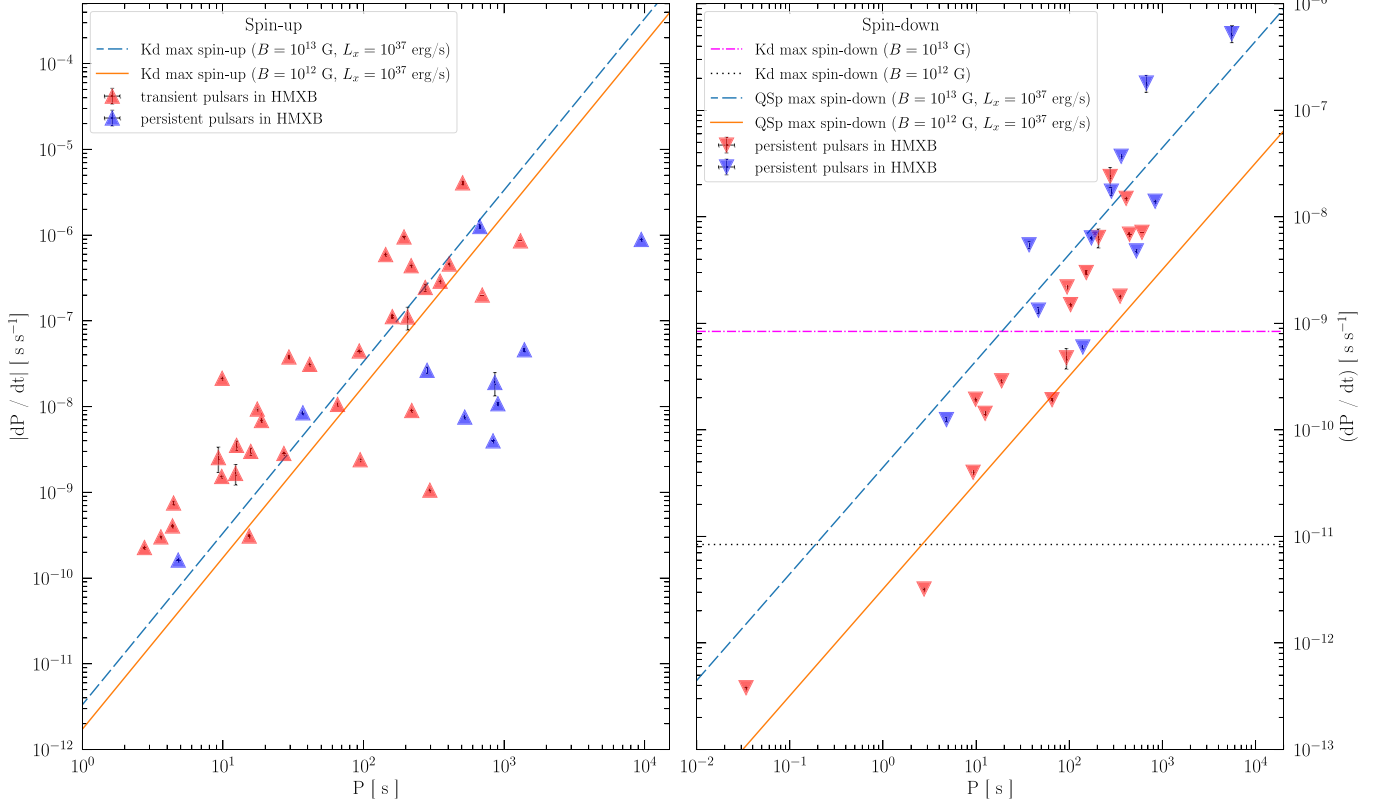


**Figure 5.**  $P_s$ - $|\dot{P}|$  diagram for Galactic X-ray pulsars in HMXBs. In the spin-up diagram (left panel), the lines correspond to the maximal possible spin-up for Kd scenario, with  $B_{ns} = 10^{13}$  G,  $L_x = 10^{37}$  erg s $^{-1}$  (dashed blue line) and with  $B_{ns} = 10^{12}$  G,  $L_x = 10^{37}$  erg s $^{-1}$  (solid orange line). In the spin-down diagram (right panel), the lines correspond to the maximal possible spin-down for the Kd scenario, with  $B_{ns} = 10^{13}$  G,  $L_x = 10^{37}$  erg s $^{-1}$  (horizontal dashed-dotted magenta line) and with  $B_{ns} = 10^{12}$  G,  $L_x = 10^{37}$  erg s $^{-1}$  (horizontal dotted line). The dashed blue line corresponds to the maximal possible spin-down for QSp, with  $B_{ns} = 10^{13}$  G,  $L_x = 10^{37}$  erg s $^{-1}$ , and the solid orange line corresponds to QSp with  $B_{ns} = 10^{12}$  G,  $L_x = 10^{37}$  erg s $^{-1}$ . Due to the high precision of the measurements, the error bars for some objects are within data points.

the NS is

$$|K| = 2\pi I \dot{\nu} = 2\pi I \frac{\dot{P}}{P_s^2}, \quad (1)$$

where  $I$  is a moment of inertia of the NS. The maximal possible value of the spin-up or spin-down torque  $|K|$  depends on the type of accretion structure surrounding an NS. In the case of accretion from a Kd, these values for spin-down (Lipunov 1982) are limited by  $|K| \leq |K_{sd}^{Kd}|$ , where

$$|K_{sd}^{Kd}| = k_t \frac{\mu_{ns}^2}{r_{cor}^3}, \quad (2)$$

and the values for spin-up (Pringle & Rees 1972) are limited by  $|K| \leq |K_{su}^{Kd}|$ , where

$$|K_{su}^{Kd}| = \dot{M} \sqrt{GM_{ns} r_A}. \quad (3)$$

Here,  $\mu_{ns} = 0.5B_{ns} R_{ns}^3$  is a dipole magnetic moment of the NS,  $r_{cor} = (GM_{ns}/\omega_s^2)^{1/3}$  is a corotation radius,  $\dot{M} = L_x R_{ns}/GM_{ns}$  is an accretion rate onto the NS surface,  $r_A = [\mu_{ns}^2/\dot{M}(2GM_{ns})^2]^{2/7}$  is the Alfvén radius,  $R_{ns}$  is a radius of the NS, and  $k_t$  is a dimensionless parameter of the order of unity. In the case of QSp, the spin-down torque is limited by

$|K| \leq |K_{sd}^{QSp}|$  (Shakura 1975), where

$$|K_{sd}^{QSp}| = k_t \dot{M} \omega_s r_A^2. \quad (4)$$

On the diagrams, corresponding lines show the borders of the maximal possible spin changes in frames of QSp and Kd accretion with the canonical parameters of an NS ( $R_{ns} = 10^6$  cm,  $M_{ns} = 1.4 M_\odot$ ,  $I = 10^{45}$  g cm $^2$ ) and a surface magnetic field  $10^{12}$ – $10^{13}$  G with upper luminosity  $L_x \sim 10^{37}$  erg s $^{-1}$  in a quiescent state. Acceptable values of ( $R_{ns}$ ,  $I$ ,  $M_{ns}$ ) for all NSs are in a narrow range close to the canonical parameters; their variations influence the evaluation insignificantly. As shown in Figure 5, some of the HMXB X-ray pulsars from the Galactic population demonstrate a spin evolution  $\dot{P}$  exceeding the Kd and QSp theoretical upper limits. See the further discussion in Section 6.

Since their discovery, and over the entire study period, X-ray pulsars' spin periods have changed insignificantly. The changes are usually a few seconds (La Palombara et al. 2009). In a very rare case, as for the pulsar 2S 0114+650, a period change value reaches several minutes, but is still  $\sim 5\%$  of its average spin period ( $P_s \simeq 9475$  s; Wang 2011). Period changes were discovered as a minimum for 52 (15 persistent and 37 transient sources) Galactic HMXB X-ray pulsars (shown in Figure 5 and listed in the catalog).

### 3.3. Magnetic Fields

There are two basic methods for estimating the surface magnetic field of an NS—namely, an X-ray pulsar. The first of

them is based on the interaction (angular momentum exchange) between the accretion flow and magnetosphere of the rotating NS (see Section 3.2 for more details and cited literature). If the spin period is known and the rate of its spin-down is observed, then from Equations (1), (2), and (3), depending on the implemented accretion scenario, one can calculate the magnetic dipole moment  $\mu_{\text{ns}}$  and then the surface magnetic field strength  $B_{\text{ns}}$ . This method essentially depends on the parameters of the models and may give contradictory results in the frameworks of various accretion scenarios (see, for example, Klus et al. 2014); therefore, it is not a reliable way for the estimation of  $B_{\text{ns}}$ .

The second method is based on spectral analysis. X-ray spectra of highly magnetized NSs may demonstrate the so-called cyclotron lines predicted by Gnedin & Sunyaev (1974). They are due to the resonant scattering of photons by electrons in a strong magnetic field of an NS. The analysis of these absorption lines allows the estimation of the surface magnetic field strength with high reliability. This method does not depend on accretion parameters and is the main one for the magnetic field estimation of X-ray pulsars (Staubert et al. 2019).

The spectra of 31 objects (6 persistent and 25 transient HMXB pulsars) demonstrate the presence of a cyclotron line. The measured surface magnetic field strength of these sources lies in a narrow range from  $\sim 0.86 \times 10^{12}$  G to  $\sim 7.8 \times 10^{12}$  G. These estimations are in good agreement with the canonical value  $B_{\text{ns}} \sim 10^{12}$  G for NSs (Lipunov 1992; Lyne & Graham-Smith 2012).

### 3.4. Massive Companions

The massive companions of transient pulsars are usually represented by main-sequence stars. In contrast, the massive companions of persistent pulsars are primarily represented by hot stars of early luminosity classes (giants and supergiants).

An interesting fact is that the massive components of the currently known HMXBs are in a relatively narrow range of spectral types, O6.5–B3, and a wide range of luminosity classes that extend from main-sequence stars to supergiants (see the catalog in Tables 2 and 3 in the Appendix). One of the possible reasons for this situation is the relatively small number of stars whose spectral type is earlier than O6.5. On the other hand, the outflow rate of stars whose spectral type is later than B3 (Puls et al. 2008; Krtička 2014) turns out to be too low to provide a sufficiently high luminosity of the accretion source (see Section 6).

## 4. Some Remarks

### 4.1. Notable Galactic HMXB Pulsars

*SAX J0635.2+0533*. This transient source has the smallest spin period  $P_s \simeq 0.0338$  s in the Galactic population of HMXB pulsars. It is comparable with those of radio pulsars (ejectors). But it is one of the unique cases in the population of X-ray pulsars in massive binary systems. Its X-ray emission is apparently due to rotation-powered processes (Pacini 1970). For the canonical parameters of an NS, in this case, a centrifugal barrier occurs, which prevents accretion or surface magnetic field from being less than  $B_{\text{ns}} \leq 10^8$  G (Mereghetti & La Palombara 2009). This value is four orders of magnitude less than expected from a young accreting NS in an HMXB system, which is doubtful.

*Swift J0243.6+6124*. The first discovered ultraluminous X-ray (ULX) pulsar in an HMXB in our Galaxy and, currently, the only known object from this class in the Galactic

population. Swift J0243.6+6124 was discovered in 2017 by Swift/Burst Alert Telescope (BAT) as a possible GRB, but further observations showed continuous X-ray flux from this object with 9.86 s periodicity. This fact indicated that the object was an accreting NS (Kennea et al. 2017). Observations in the optical range allowed us to identify its normal companion—an O9.5Ve star at  $\sim 5$  kpc distance (Reig et al. 2020). The distinguishing feature of this pulsar is its ultrahigh X-ray luminosity, reaching  $> 10^{39}$  erg s $^{-1}$  during outburst activity, exceeding the Eddington limit, but in the quiescent state, it dropped to  $(0.3\text{--}6) \times 10^{34}$  erg s $^{-1}$  (Doroshenko et al. 2020b). To explain the ULX phenomenon, there are several possible hypotheses. (1) The presence of a multipolar magnetic field of the NS with superstrong  $B_{\text{ns}} \geq 10^{14}$  G. In this case (Israel et al. 2017), the high radiation flux will not block its accretion flow totally. (2) In Mushtukov et al. (2015), ULX pulsars and the super-Eddington accretion phenomenon are explained by the specific geometry of the accretion column, where generated photons can escape not only in a radial direction (along the column), but also through the sides of the column. This approach also implies the presence of a superstrong  $B_{\text{ns}} \geq 10^{14}$  G magnetic field on the NS surface. However, at the moment, there is no evidence of the presence of a superstrong magnetic field in the Galactic population of HMXB pulsars (see the catalog Table 3 in the Appendix).

*X Per (X Persei, 4U 0352+309)*. This persistent pulsar has a large absolute galactic latitude  $|b| \simeq 17^\circ 1$  (see Figure 2) as compared to other HMXB pulsars not exceeding  $4^\circ 1$  from the galactic plane. The large galactic latitude of X Per can be explained either by the “binary supernova mechanism” or “dynamical ejection” (Raddi et al. 2021). The first one points to a mechanism of runaway through a supernova explosion in a binary system. The second possibility can occur in few-body interactions in clusters when binding energy transforms into kinetic energy (Oh & Kroupa 2016). In both cases, there is a high probability of system decomposition (Oh & Kroupa 2016; Raddi et al. 2021). Still, an NS and a normal component could form a binary system after gravitational capture has occurred after the escape from the Galactic plane.

*SGR 0755-2933*. This object was discovered by the Swift Burst Alert Telescope in 2016 as a short ( $< 128$  ms) and spectrally soft gamma-ray burst without detected optical afterglow. The source is located in the Galactic plane ( $b \sim -0.6$  deg; Barthelmy et al. 2016). Initially, the source was assumed to be a soft gamma repeater (SGR)—an isolated magnetized NS with nonperiodic burst activity. Further observations by Swift/X-Ray Telescope (XRT), NuSTAR, and Chandra revealed the presence of modulations in the X-ray flux of SGR 0755-2933 associated with spin rotation and orbital motion in a massive binary system. Therefore the initial assumption about the isolated origin of this object was disproved (Doroshenko et al. 2021). However, the prefix “SGR” was saved for this HMXB pulsar.

*2S 0114+650*. This persistent pulsar has the second-longest spin period ( $P_s \simeq 9475$  s; Wang 2011) among Galactic HMXB pulsars. For most of the known X-ray pulsars in HMXBs, especially persistent sources, their spin periods exceed  $P_s > 100$  s, but are less than 1000 s. Compared with radio pulsars, whose spin periods usually do not exceed 1 s, HMXB X-ray pulsars are long-periodic. This phenomenon is related to the spin evolution of a magnetized NS from ejector to accretor with an intermediate propeller stage (Lipunov 1992). Since the

discovery of 2S 0114+650, its global spin-up trend with a high rate  $\sim 10^{-6}$  s s $^{-1}$  (see the catalog) has been observed (Bonning & Falanga 2005). The origin of its ultralong spin period and high-rate spin-up are still unknown.

*AX J1910.7+0917.* This transient pulsar has the longest spin period among all known pulsars, including other populations: low-mass X-ray binaries (LMXBs), radio pulsars (RPs), anomalous X-ray pulsars (AXPs), soft gamma repeaters (SGRs), etc. The object was discovered as a Galactic faint X-ray source during the ASCA Galactic Plane Survey (Sugizaki et al. 2001), carried out from 1996 to 1999. Further photometric and spectral observations in the near-infrared range with the 3.58 m Telescopio Nazionale Galileo at Roque de los Muchachos Observatory (La Palma, Spain) made it possible to identify the optical counterpart as a massive B-class supergiant located at a distance  $16.0 \pm 0.5$  kpc. A timing analysis of its X-ray flux from observations performed in 2011 by the Chandra space observatory showed evident periodic modulations with  $P_s = 36200 \pm 110$  s (Sidoli et al. 2017), which was identified as an NS spin period. According to Sidoli et al. (2017), the anomalously long period of AX J1910.7+0917 could be explained in the frame of QSp. Assuming a stellar wind velocity  $v_w = 1000$  km s $^{-1}$ , surface magnetic field  $B_{ns} = 10^{12}$  G, and orbital period  $P_{orb} = 68$  days, a canonical NS accreting in the QSp regime can spin down to 36,200 s on a  $\tau \sim 10^4$  yr timescale. But the question remains: why do other HMXB pulsars with similar parameters not reach identically long spin periods?

#### 4.2. Some Candidates for HMXB X-Ray Pulsars

We provide information on candidates of HMXB pulsars (the green diamonds in Figure 2). The list has been formed from the candidate objects of the studied catalogs (Liu et al. 2006; Fortin et al. 2023; Krivonos et al. 2022; Neumann et al. 2023) and extensively searched for additional information via SIMBAD and the literature. Candidates are of interest for further attentive investigation.

##### 4.2.1. Pulsar Candidates with Unclear Spin Period

*IGR J14488-5942.* This object was discovered in 2009 by Swift/XRT as an X-ray point source (Landi et al. 2009). A period of  $49.51 \pm 0.12$  days was found by analyzing the amplitude modulation in the IGR J14488-594 light curve (covering the 2005–2009 interval in the 15–100 keV range received from Swift/BAT). The period was expected to be the system's orbital period (Corbet et al. 2010a). Based on optical and near-infrared spectral and photometric observations on a 3.58 m telescope (ESO/New Technology Telescope, Chile), it was supposed that the system corresponded to an HMXB with an Oe/Be optical counterpart (Coleiro et al. 2013). According to Corbet et al. (2017), there are some hints of possible pulsations with period  $33.419 \pm 0.001$  s, but this needs further investigation.

*IGR J19140+0951.* This X-ray source was discovered in 2003 by INTEGRAL (Swank & Markwardt 2003). Near-infrared photometric observations on a 3.58 m telescope (Roque de los Muchachos Observatory/Telescopio Nazionale Galileo, La Palma, Spain) showed that the IGR J19140+0951 optical counterpart could be a B0.5 supergiant (Iab luminosity class) located at a distance of  $3.6 \pm 0.04$  kpc (Torrejón et al. 2010), confirming an HMXB status. According to Sidoli et al. (2016), XMMNewton observations of IGR J19140+0951 performed in 2015 showed quasiperiodic oscillations of X-ray flux (2–10 keV

range) with a  $5937 \pm 219$  s period, which could be associated with the NS spin period, but this needs further investigation.

##### 4.2.2. Pulsar Candidates with Unclear Status of Optical Counterpart

*SAX J1452.8-5949, AX J1700.1-4157, and IGR J16358-4726.* Three Galactic X-ray pulsars in binary systems. SAX J1452.8-5949 and AX J1700.1-4157 were discovered in 1999 by BeppoSAX and ASCA, correspondingly. Initially, their origins were considered as X-ray pulsars in high-mass binary systems. But further detailed near-infrared and optical identification showed that their normal companions were late-type low-mass stars, thus SAX J1452.8-5949 and AX J1700.1-4157 were classified as LMXBs (Kaur et al. 2009, 2010b), therefore the objects were not included in our catalog. However, both objects in the SIMBAD database and AX J1700.1-4157 in Fortin's and Neumann's catalogs are marked as HMXBs. A similar history takes place with IGR J16358-4726. This object was discovered in 2003 by Chandra as a point X-ray source with  $P_s \simeq 5860$  s periodicity (Kouveliotou 2002). Over the next decade, there was a discussion about its possible optical companion. D'Amico et al. (2006), based on near-infrared photometric observations on a 1.6 m telescope (Laboratorio Nacional de Astrofísica, Brazil), supposed that the system corresponded to an HMXB, but Nespoli et al. (2010), based on infrared medium-resolution spectroscopy using a UT-1 telescope (ESO), showed that the optical companion belonged to late-type (K–M) giant, thereby classifying IGR J16358-4726 as an LMXB. But the question about the spectral classification of IGR J16358-4726's optical companion is still controversial: some articles provide arguments in favor of the HMXB hypothesis (see, e.g., Coleiro et al. 2013), but also there are arguments for its LMXB origin (see, e.g., Yungelson et al. 2019). Therefore, IGR J16358-4726 as an object with unclear status was not included in our catalog.

## 5. About the Catalog Tables

The catalog is split into two parts (tables): persistent and transient sources (see Tables 2 and 3 in the Appendix). Catalog objects are arranged in ascending order of their spin periods. The first column displays the serial number of the pulsar. In the second column is its name. The third double column shows the equatorial coordinates, R.A., and decl. for the J2000 epoch from the SIMBAD Database (Wenger et al. 2000), rounded to hundredths of arcseconds. The fourth column contains the values of the spin period ( $P_s$ ) in seconds. In parentheses, we indicate the year when the given  $P_s$  was measured. Also, in the third column, under the value of the spin period, are given the changes in spin periods (rotational evolution): Loc.spin-up/down episodes (local trends) of the spin-up/spin-down of rotation and Glob.spin-up/down long-term (global) trends of the spin-up/spin-down of the pulsar's rotation. The fifth column ( $\dot{P}$ ) gives their values in units (s s $^{-1}$ ), as well as the epoch of their observations in MJD. The sixth column shows the values of the orbital periods ( $P_{orb}$ ) in days. The seventh column gives estimates of the X-ray luminosity and the range of its variations ( $L_x(\text{erg s}^{-1})$ ) in the indicated energy range (keV). The eighth column shows the value of the magnetic field strength on the surface of the NS  $B_{ns} (\times 10^{12}$  G) obtained from the analysis of cyclotron lines. The ninth column contains estimates of distances to objects (dist) in kiloparsecs. The tenth column lists information about massive companions: the first line is the star's name (or catalogued number), if available; the

second line shows the spectral types and luminosity classes; the bottom lines contain data about photometric magnitudes in the optical (*BVR*) and near-infrared (*JHK*) passbands and also values of color excess  $E(B - V)$ , if available. The corresponding references support the values of all the parameters of the X-ray pulsars given in the catalogs. All catalog data are given with the same precision as in the cited literature. In the case of different values coexisting for the same object, we used the newest data possible. The first object in Table 3 in the Appendix (SAX J0635.2+0533) is a transient X-ray pulsar with a spin period of less than 1 s. It seems to have a nonaccreting origin of X-ray radiation (Mereghetti & La Palombara 2009); therefore, it is separated from the other objects in the table by a double line.

## 6. Discussion and Summary

The main issues of finding all pulsars exclusively by the coordinate crossmatching method are related to the mismatching of coordinates due to the measurement precisions of different instruments, as well as different namings of objects. While managing to minimize the divergence and make the data uniform, the reference catalogs still inherit some inconsistencies, making a batch comparison less efficient. This required us to search for objects manually after applying the basic selection criteria. The coordinates were different enough when the search radius increased during the crossmatching; false matches began to quickly appear in TOPCAT. These false match cases have to be examined individually, because the name search was complicated too. Some of the names in different directories are used differently and it is necessary to inspect them in SIMBAD, where multiple names can exist for the same object. We found 19 additional HMXB pulsars in the supplementary sectors of Figure 1 in two pairs of the three catalogs (Fortin–Neumann: 16 objects; Krivonos–Neumann: one object) and two single catalogs (Krivonos: one object; Neumann: one object).

The number of known transients significantly exceeds those of persistent sources, 64 versus 18 ( $\sim 3.6$  times), in the Galactic population of HMXB pulsars. This is explained by transients mostly having orbits with a significant eccentricity, found in a wide range from 0.2 and reaching 0.9, while for most of the persistent pulsars, the eccentricity does not exceed 0.2 (Fortin et al. 2023). According to the evolution of close massive binary systems, during HMXB formation, one of the massive companions normally ends its life with a core collapse followed by a supernova explosion. It significantly changes the orbital parameters of the system, including an increase of eccentricity (van den Heuvel 2017; Tutukov & Cherepashchuk 2020). Thus, an NS born in a high-mass binary system is more likely to have an orbit with a relatively high value of eccentricity. This, in turn, leads to transient X-ray activity, due to the dynamic increase of the accretion rate during its orbital motion from apoaster to periaster (Negueruela 1998).

The massive components of the currently known Galactic HMXB pulsars are in a relatively narrow range of spectral types O6.5–B3; see the last column of the catalog tables. One of the possible reasons for this situation is the relatively small number of stars whose spectral type is earlier than O6.5. The number of O-class stars in the Galaxy (including all subclasses) lies within  $\sim(1.8\text{--}5)\times 10^4$ , and it does not exceed one-tenthousandth of a percent of the Galactic star population (Maíz Apellániz et al. 2013). On the other hand, the outflow rate of stars whose spectral type is later than B3 turns out to be too low

to provide a sufficiently high luminosity of the accretion source. As mentioned in Krtička (2014) and Puls et al. (2008), the mass-loss rate of B-class stars rapidly decreases as the subclass goes from B0 to B9; moreover, for the B5 subclass and later, the stellar wind is not homogeneous.

As shown in Figure 5, the spin changes (spin-up and spin-down) for some of the Galactic X-ray pulsars in HMXBs significantly exceed the maximal possible values predicted within classical accretion scenarios, QSp and accretion from Kd. Isolated cases of this phenomenon were already known in the early era of X-ray astronomy (Shakura 1975). The number of such cases even increased over time, as new sources were discovered and data accumulated (see Figure 5). One possible explanation for the rapid spin evolution can be the formation of non-Keplerian accretion structures surrounding an NS in an HMXB. As was shown in Ikhsanov & Finger (2012) and Ikhsanov & Mereghetti (2015), the presence of magnetized stellar wind from a massive companion can influence the structure of the accretion with the formation of a non-Keplerian magnetically arrested disk (MAD-disk or ML-disk). In this case, the angular momentum exchange between an accretion flow and an NS can be more efficient than the QSp and Kd scenarios.

In summary, we have carried out work on searching and identifying Galactic X-ray pulsars in HMXB systems by cross-matching various catalogs and databases. We created a catalog of X-ray pulsars with 82 sources, consisting of 18 persistent pulsars and 64 transients. The catalog contains individual information for each object: its period and evolution, orbital period, X-ray luminosity in the indicated energy range, magnetic field strength, distance, and the characteristics of a massive component. We provide Table 2 in the Appendix, with 18 persistent pulsars in HMXBs, and Table 3 in the Appendix, with 64 transient pulsars in HMXBs, in a machine-readable format.

## Acknowledgments

This research has been funded by the Science Committee of the Ministry of Education and Science of the Republic of Kazakhstan (grant No. AP09258811). We thank Dr. Francis Fortin for the useful discussion on methods. I.I. acknowledges the efficient training on VO tools and services given at the Second ESCAPE-VO School, funded by the European Union’s Horizon 2020—grant No. 824064 (ESCAPE Project). The authors acknowledge the editor and anonymous referees for comments and suggestions that improved the presentation of the results.

This research has made use of data and/or software provided by the High Energy Astrophysics Science Archive Research Center (HEASARC), which is a service of the Astrophysics Science Division at NASA/GSFC. This research has made use of the SIMBAD database, operated at CDS, Strasbourg, France (Wenger et al. 2000). This research has made use of NASA’s Astrophysics Data System.

*Software:* NumPy (Harris et al. 2020), pandas (McKinney 2010), Astropy (Astropy Collaboration et al. 2013, 2018, 2022), TOPCAT (Taylor 2005), Matplotlib (Hunter 2007).

## Appendix

A catalog of the Galactic population of X-ray pulsars in high-mass X-ray binary (HMXB) systems is presented. It contains information about 82 confirmed sources: 18 persistent and 64 transient pulsars. The catalog is split into two parts: persistent (Table 2) and transient (Table 3) sources. Catalog objects are arranged in ascending order of their spin periods.

**Table 2**  
Catalog of Galactic Population of Persistent Pulsars in HMXB Systems

No.	Name	Eq. Coord. J2000		$P_s$ (s) Spin and Its Evol.	$\dot{P}$ (s s $^{-1}$ ) MJD	$P_{\text{orb}}$ (days)	$L_x$ (erg s $^{-1}$ ) Range (keV)	$B_{\text{ns}} (\times 10^{12} \text{ G})$	dist (kpc)	Comp. Name Spec. Class and Photom.	
		R.A.	Decl.								
1	4U 1119-603 (Cen X-3)	11:21:15.09 (2016) [1]	-60:37:25.63 (1.25 ± 0.07)E-10 [7] MJD → 56834–56857 Loc.spin-up → (-1.62 ± 0.02)E-10 [7] MJD → 56263–56315 Glob.spin-up → (-2.26 ± 0.01)E-11 [7–9] MJD → 40960–57220	4.80188 ± 85E-6 (2016) [1]	2.033 ± 0.029 [1]	(0.058–1.4)E37 1–10 [2] [3]	2.4–3 [4]	5.7 ± 1.5	V779 Cen O6.5 II–III [5] B 14.37, V 13.30 [6] J 10.736, H 10.311 K 10.093 [6] $E(B - V) 1.40$ [6]	...	
2	OAO 1657-415	17:00:48.88 (2019) [10]	-41:39:21.46 Loc.spin-down → (5.46 ± 0.39)E-9 [14] MJD → 56188–56283 Loc.spin-up → (-8.46 ± 0.13)E-9 [14] MJD → 55192–55365 Glob.spin-up → (-1.08 ± 0.01)E-9 [8],[9],[14],[15] MJD → 43756–57250	37.024578 ± 5E-6 [11]	10.44729 ± 21E-4 1–10 [2] [2]	(0.1–2)E37 [12]	3.29 ± 0.23 [12]	6.4 ± 1.5	Ofpe/WNL [13] J 14.09 ± 0.05, H 11.68 ± 0.04 K 10.38 ± 0.04 [13a]	...	
3	IGR J22534+6243	22:53:55.13 (2009) [16]	62:43:36.79 Loc.spin-down → (1.33 ± 0.09)E-9 [16] MJD → 54937–54959 Glob.spin-down → ~5.3E-10 [16] MJD → 48988–55561	46.6784 ± 37E-3 [16]	>22 [16] 17–60 [16]	~3E34 [16]	...	9.7 ± 1.7	B0–1 III–Ve [16] B 17.38 ± 0.1, V 15.78 ± 0.09 [16] R 13.3, I 13.29 [13a] J 11.64 ± 0.02, H 10.96 ± 0.02 K 10.46 ± 0.03 [16]	...	
4	IGR J18027-2016	18:02:39.90 (2015) [17]	-20:17:13.00 Glob.spin-down → ~6E-10 [19] MJD → 52640–57387	139.866 ± 0.001 [19]	4.5696 ± 9E-4 1–10 [2]	(0.27–1.3)E37 [17]	~3 [18]	12.4 ± 0.1	B1 Ib [18] J 12.79 ± 0.06, H 11.96 ± 0.08 K 11.48 ± 0.05 [18] $E(B - V) 3.04 ± 0.02$ [18]	...	
5	SAX J1324.4-6200	13:24:26.70 (2008) [20]	-62:01:19.50 Glob.spin-down → (6.34 ± 0.08)E-9 [20] MJD → 49353–54831	172.86 ± 0.02 [20a]	1.1250 ± 0.0417 1–10 [21]	~1.1E34 [21]	...	>3.4	...	Be [20]	

**Table 2**  
(Continued)

No.	Name	Eq. Coord. J2000		$P_s$ (s) Spin and Its Evol.	$\dot{P}$ (s s $^{-1}$ ) MJD	$P_{\text{orb}}$ (days)	$L_x$ (erg s $^{-1}$ ) Range (keV)	$B_{\text{ns}} (\times 10^{12} \text{ G})$	dist (kpc)	Comp. Name Spec. Class and Photom.
		R.A.	Decl.							
6	4U 0900-40 (Vela X-1)	09:02:06.86	-40:33:16.90	$283.4290 \pm 6\text{E-}4$ (2013) [25]		$8.964368 \pm 4\text{E-}5$ [23]	$(0.0061\text{--}1)\text{E}37$ 1–10 [2]	~2.6 [25]	$1.9 \pm 0.2$ [26]	HD 77581 B0.5 Ia [27] B 7.37, V 6.87 R 6.31, I 6.05 [28a] J 5.833 ± 0.020, H 5.705 ± 0.034 K 5.596 ± 0.024 [13a] $E(B - V)$ $0.689 \pm 0.018$ [28b]
				Loc.spin-down →	$(1.74 \pm 0.16)\text{E-}8$ [28]					
				MJD →	54770–54803					
				Loc.spin-up →	$(-2.65 \pm 0.26)\text{E-}8$ [28]					
				MJD →	54806–54844					
				Glob.spin-down →	$(8.55 \pm 0.19)\text{E-}10$ [8],[9]					
				MJD →	42449–51343					
				Glob.spin-up →	$(-3.34 \pm 0.13)\text{E-}10$ [28]					
				MJD →	54690–57217					
7	XTE J1855-026	18:55:30.41	-02:36:16.74	$360.741 \pm 0.002$	...	$6.0724 \pm 9\text{E-}4$	$(0.21\text{--}1.9)\text{E}37$	...	~10	...
						[30]	1–10 [2]		[29]	
				(2006) [30a]						B0 Iaep [29a]
				Loc.spin-down →	$\sim 3.7\text{E-}8$ [30]					J 10.564 ± 0.026, H 10.089 ± 0.024
				MJD →	?					K 9.799 ± 0.021 [13a]
12	EXO 1722363	17:25:11.39	-36:16:57.53	$413.7 \pm 0.3$ (2004) [31]	...	$9.7403 \pm 4\text{E-}4$ [32]	$(0.47\text{--}9.2)\text{E}36$ 20–60 [33]	...	7.1–7.9 [33]	...
										B0–1 Ia [33]
										V 14.3 ± 0.1 [33a]
										J 14.218 ± 0.035, H 11.811 ± 0.028
										K 10.672 ± 0.026 [13a]
9	4U 1538-52	15:42:23.36	-52:23:09.58	$526.41 \pm 0.07$ (2016) [33a]		$3.72831 \pm 2\text{E-}5$ [33a]	$(0.42\text{--}4.3)\text{E}36$ 1–10 [2]	2.1–2.3 [34]	$5 \pm 0.5$ [2]	QV Nor B0.2 Ia [36]
				Glob.spin-up →	$(-7.54 \pm 0.16)\text{E-}9$ [8],[9]					B 16.3, V 14.5 [35]
				MJD →	47223–51315					J 10.358 ± 0.025, H 9.910 ± 0.023
				Glob.spin-down →	$(4.79 \pm 0.12)\text{E-}9$ [37]					K 9.677 ± 0.022 [13a]
				MJD →	54690–57220					$E(B - V)$ 2.10 [6]
10	4U 1223-624 (GX 301-2)	12:26:37.56	-62:46:13.26	$672.51 \pm 0.05$ (2019) [38]		$41.508 \pm 0.007$ [39]	$(0.023\text{--}3)\text{E}37$ 1–10 [2]	3.4–4.2 [41]	$3.5 \pm 0.5$ [2]	BP Cru B1.5 Ia [40]
				Loc.spin-down →	$(1.80 \pm 0.33)\text{E-}7$ [42]					B 12.70 ± 0.36, V 10.66 ± 0.07 [42a]
				MJD →	55094–55122					J 6.717 ± 0.021, H 6.077 ± 0.029
				Loc.spin-up →	$(-1.26 \pm 0.08)\text{E-}6$ [42]					K 5.672 ± 0.017 [13a]
				MJD →	55354–55402					$E(B - V)$ 1.84 [6]
				Glob.spin-down →	$(1.30 \pm 0.01)\text{E-}8$ [9],[42]					
				MJD →	49324–57222					

**Table 2**  
(Continued)

No.	Name	Eq. Coord. J2000		$P_s$ (s) Spin and Its Evol.	$\dot{P}$ (s s $^{-1}$ ) MJD	$P_{\text{orb}}$ (days)	$L_x$ (erg s $^{-1}$ ) Range (keV)	$B_{\text{ns}} (\times 10^{12} \text{ G})$	dist (kpc)	Comp. Name Spec. Class and Photom.
		R.A.	Decl.							
		Glob.spin-up →		( $-3.67 \pm 0.17$ )E-8 [8],[9]						
		MJD →		42417–49200						
11	4U 0352+309 (X Per)	03:55:23.08	31:02:45.04	$835.29 \pm 0.29$ (2012) [43]		$250.3 \pm 0.6$ [44]	(1.2–6.3)E34 1–10 [2]	$\sim 5.6$ [46]	$0.801 \pm 0.138$ [44a]	HD 24534 B0 Ve [45] $B 6.840 \pm 0.007, V$ $6.720 \pm 0.009$ [47a] J $6.149 \pm 0.018, H$ $6.073 \pm 0.024$ K $5.920 \pm 0.016$ [13a] $E(B - V)$ $0.356 \pm 0.003$ [47b]
		Loc.spin-down →		$\sim 1.4\text{E-}8$ [47]						
		MJD →		43413–43532						
		Glob.spin-up →		( $-3.98 \pm 0.03$ )E-9 [44]						
		MJD →		42778–44969						
		Glob.spin-down →		$\sim 3.45\text{E-}9$ [46]						
		MJD →		44000–50000						
12	4U 1036-56	10:37:35.31	–56:47:55.87	$860 \pm 2$ (1998) [48]		$61 \pm 0.2$ [49]	(2–4.5)E35 3–30 [48]	...	$\sim 5$ [50]	LS 1698 B0 V–IIIe [50] $B 12.00 \pm 0.03, V$ $11.48 \pm 0.03$ R $11.38 \pm 0.04$ [51a] J $10.122 \pm 0.024, H$ $9.954 \pm 0.022$ K $9.891 \pm 0.023$ [13a] $E(B - V) 0.75 \pm 0.25$ [51b]
		Glob.spin-up →		( $-1.91 \pm 0.58$ )E-8 [51]						
		MJD →		51179–55196						
13	Swift J2000.6+3210	20:00:21.86	32:11:23.13	$887.6 \pm 2.8$ (2006) [51c]		...	(2–4)E35	...	$\sim 8$	...
						0.3–10 [51c]		[51d]		B V–III [51d] V $13.20 \pm 0.09$ [51e] R $16.1$ [51d] J $11.953 \pm 0.021, H$ $11.290 \pm 0.019$ K $10.847 \pm 0.018$ [13a]
14	IGR J16393-4643	16:39:05.50	–46:42:14.00	$904.0 \pm 0.1$ (2014) [54]		$\sim 4.2378472$	(5.2–9.9)E35	$2.5 \pm 0.1$	$\sim 10$	...
		Glob.spin-up →		( $-1.08 \pm 0.03$ )E-8 [53]		[54a]	1–10 [2]	[54]	[52]	Be V [55]
		MJD →		53215–53815						
15	IGR J16493-4348	16:49:26.95	–43:49:09.00	$1093.1036 \pm 4\text{E-}4$ (2019) [56]	...	$6.7828 \pm 4\text{E-}4$ [56]	(0.9–2.4)E36 1–10 [57]	$3.7 \pm 0.4$ [58]	$16.1 \pm 1.5$ [56]	...
										B0.5 Ia [56] J $14.595 \pm 0.054, H$ $12.859 \pm 0.056$ K $11.935 \pm 0.038$ [13a]

**Table 2**  
(Continued)

No.	Name	Eq. Coord. J2000		$P_s$ (s) Spin and Its Evol.	$\dot{P}$ (s s $^{-1}$ ) MJD	$P_{\text{orb}}$ (days)	$L_x$ (erg s $^{-1}$ ) Range (keV)	$B_{\text{ns}} (\times 10^{12} \text{ G})$	dist (kpc)	Comp. Name Spec. Class and Photom.
		R.A.	Decl.							
16	RX J0146.9+6121	01:47:00.21	61:21:23.66	$1396.14 \pm 0.25$  (2006) [60] Glob.spin-up → MJD →	$(-4.6 \pm 0.2)\text{E-}8$ [60] 45700–53370	$\sim 330$ [61]	$(1\text{--}1.1)\text{E}35$ 1–10 [2]	...	$2.3 \pm 0.5$ [62]	V831 Cas  B1 Ve [62a] B 12.09, V 11.42 R 11.00, I 10.52 [62a] J $9.899 \pm 0.027$ , H 9.700 ± 0.036 K $9.486 \pm 0.020$ [13a] $E(B - V)$ $0.88 \pm 0.03$ [62a]
17	4U 2206+54	22:07:56.24	54:31:06.41	$5554 \pm 9$  (2010) [63] Glob.spin-down → MJD →	$(5.24 \pm 0.93)\text{E-}7$ [63] 51141–54237	$19.25 \pm 0.8$ [64]	$(1.3\text{--}6.7)\text{E}35$ 1–10 [2]	$\sim 3.3$ [65]	$3.0 \pm 0.7$ [62a]	BD+53 2790  O9.5Ve [62a] B 10.11, V 9.84 R 9.64, I 9.43 [62a] J $9.218 \pm 0.025$ , H 9.116 ± 0.027 K $9.038 \pm 0.022$ [13a] $E(B - V)$ $0.51 \pm 0.03$ [62a]
14	2S 0114+650	01:18:02.70	65:17:29.83	$9475 \pm 25$  (2008) [67] Glob.spin-up → MJD →	$\sim 8.9\text{E-}7$ [69] 50451–53348	$11.591 \pm 0.003$ [68]	$(0.067\text{--}1.2)\text{E}37$ 1–10 [2]	$\sim 2.5$ [69]	$5.9 \pm 1.4$ [70]	V662 Cas  B1 Ia [70] B 12.17, V 11.03 R 10.33, I 9.58 [62a] J $8.597 \pm 0.026$ , H 8.296 ± 0.034 K $8.107 \pm 0.024$ [13a] $E(B - V)$ $1.33 \pm 0.04$ [62a]

#### Note.

References for Table 2: (1) Shirke et al. (2021); (2) Sidoli & Paizis (2018); (3) Santangelo et al. (1998); (4) Thompson & Rothschild (2008); (5) Hutchings et al. (1979); (6) Liu et al. (2006); (7) Fermi Collaboration (2021c; Cen X-3); (8) Nagase (1989); (9) CGRO Collaboration (2000); (10) Falanga et al. (2015); (11) Jenke et al. (2012a); (12) Chakrabarty et al. (2002); (13) Mason et al. (2009); (13a) Cutri et al. (2003); (14) Fermi Collaboration (2021); OAO 1657-415; (15) Barnstedt et al. (2008); (16) Esposito et al. (2013); (16a) Fortin et al. (2023); (17) Lutovinov et al. (2017); (18) Torrejón et al. (2010); (19) Hill et al. (2005); (20) Kaur et al. (2009); (20a) Lin et al. (2002); (21) Angelini et al. (1998); (23) Quaintrell et al. (2003); (25) Fürst et al. (2014a); (26) Sadakane et al. (1985); (27) Houk (1978); (28) Fermi Collaboration (2021); Vela X-1; (28a) Ducati (2002); (28b) Kretschmar et al. (2021); (29) Corbet et al. (1999); (29a) Negueruela et al. (2008); (30) Corbet & Mukai (2002); (30a) Bodaghee et al. (2007); (31) Zurita Heras et al. (2006); (32) Thompson et al. (2007); (33) Mason et al. (2010); (33a) Hemphill et al. (2019b); (34) Hemphill et al. (2013); (35) Maccarone et al. (2014); (36) Parkes et al. (1978); (37) Fermi Collaboration (2021b); 4U 1538-52; (38) Nabizadeh et al. (2019a); (39) Sato et al. (1986); (40) Kaper et al. (1995); (41) Kreykenbohm et al. (2004); (42) Fermi Collaboration (2021f; GX 301-2); (42a) Högl et al. (2000); (43) Maitra et al. (2017); (44) Delgado-Martí et al. (2001); (44a) Bodaghee et al. (2012b); (45) Lyubimkov et al. (1997); (46) Di Salvo et al. (1998); (47) Ichsanov et al. (2014); (47a) Oja (1991); (47b) Nikolov et al. (2017); (48) Reig & Roche (1999); (49) Cusumano et al. (2013); (50) Motch et al. (1997); (51) La Palombara et al. (2009); (51a) Zacharias et al. (2012); (51b) Sarty et al. (2011); (51c) Pradhan et al. (2013); (51d) Masetti et al. (2008); (51e) Alfonso-Garzón et al. (2012); (52) Bodaghee et al. (2006); (53) Thompson et al. (2006); (54) Bodaghee et al. (2016); (54a) Islam et al. (2015); (55) Chaty (2008); (56) Pearlman et al. (2019); (57) Coley et al. (2019); (58) D'Ai et al. (2011); (60) La Palombara & Mereghetti (2006); (61) Sarty et al. (2009); (62) Reig et al. (1997); (62a) Reig & Fabregat (2015); (63) Finger et al. (2010); (64) Corbet et al. (2007); (65) Torrejón et al. (2004); (67) Wang (2011); (68) Corbet & Krimm (2013); (69) Bonning & Falanga (2005); and (70) Reig et al. (1996).

(This table is available in machine-readable form.)

**Table 3**  
Catalog of Galactic Population of Transient Pulsars in HMXB Systems

No.	Name	Eq. Coord. J2000		$P_s$ (s) Spin and Its Evol.	$\dot{P}$ (s s <sup>-1</sup> ) MJD	$P_{\text{orb}}$ (days)	$L_x$ (erg s <sup>-1</sup> ) Range (keV)	$B_{\text{ns}} (\times 10^{12} \text{ G})$	dist (kpc)	Comp. Name Spec. Class and Photom.
		R.A.	Decl.							
1	SAX J0635.2+0533	06:35:17.40	05:33:21.00	$0.0338565 \pm 1E-7$ (1997) [71]		$11.2 \pm 0.5$ [72]	(3–27.6)E32 0.2–12 [74]	...	2.5–5 [73]	B1–2 IIe–Ve [75] B 13.81, V 12.83 R 11.98 [73] $E(B - V) 1.2 \pm 0.2$ [73]
				Loc. spin-down → MJD →	$\sim 3.8E-13$ [72] 51417–51420					
2	4U 1901+03	19:03:39.39	03:12:15.76	$2.761 \pm 0.001$ (2019) [76]		$22.5827 \pm 2E-4$ [77]	(0.27–1.9)E37 1–10 [2]	...	>10 [77]	...
				Loc. spin-up → MJD →	$(-2.272 \pm 3E-4)E-10$ [77] 52680–52837					Be [79]
				Glob. spin-down → MJD →	$\sim 3.21E-12$ [78] 55914–58522					J 14.138 ± 0.028, H 13.220 ± 0.033 K 12.581 ± 0.028 [13a]
3	4U 0115+634	01:18:31.97	63:44:33.07	$3.61398 \pm 2E-5$ (2017) [80]		$24.31643 \pm 7E-5$ [81]	(0.099–3.7)E37 1–10 [2]	~1 [82]	6 ± 1.5 [62a]	V635 Cas B0.2 Ve [83] B 16.92, V 11.03 R 14.34, I 13.22 [62a] $E(B - V) 1.71 \pm 0.05$ [62a]
				Glob. spin-up → MJD →	$(-8.36 \pm 0.04)E-11$ [84] 44605–54831					
				Loc. spin-up → MJD →	$(-3.02 \pm 0.01)E-10$ [84] 54555–54566					
4	V 0332+53	03:31:14.87	53:00:24.20	$4.3748 \pm 9E-5$ (2005) [86]		$34.67 \pm 0.38$ [86]	(0.094–6.4)E37 1–10 [2]	~2.5 [87]	6 ± 1.5 [62a]	BQ Cam O8.5 Ve [88] B 17.16, V 15.42 R 14.26, I 13.04 [62a] J 11.817 ± 0.023, H 11.21 ± 0.03 K 10.744 ± 0.025 [13a] $E(B - V) 1.94 \pm 0.03$ [62a]
				Loc. spin-up → MJD →	$(-4.05 \pm 0.11)E-10$ [86] 53367–53392					
15	GRO J1750-27	17:49:12.97	-26:38:38.93	$4.451271 \pm 2E-6$ (2022) [90]		$29.817 \pm 0.009$ [91]	(0.78–8.5)E37 1–10 [2]	~3.7 [90]	>12 [91a]	...
				Loc. spin-up → MJD →	$(-7.5 \pm 0.3)E-10$ [92] 54507–54576					Be [91]
6	AX J1841.0-0536	18:41:00.43	-05:35:46.50	$4.7394 \pm 8E-4$ (1999) [93]	...	~25 [93]	(0.023–1.1)E36 2–10 [93]	...	3.2 ± 2 [94]	...
										B1 Ib [94] K 8.9 [94]
7	XTE J1829-098	18:29:44.01	-09:51:23.00	$7.8448 \pm 2E-5$ (2018) [95]	...	$244.2 \pm 0.2$ [95a]	3E32–3E36 2–10 [96]	~1.7 [95]	4.5–18 [97]	...
										Bo V–Bo.5 Ib [97] J 16.147 ± 0.009, H 14.064 ± 0.003 K 12.591 ± 0.002 [96a]
8	2S 1553-542	15:57:49.00	-54:24:54.00	$9.27949 \pm 8E-6$ (2021) [97a]		$31.303 \pm 0.027$ [98]	1.1E34–3.2E37 0.5–10 [97b]	~3 [98]	>15 [97b]	...
				Loc. spin-up → MJD →	$(-2.54 \pm 0.83)E-9$ [97c] 54480–54540					J 15.78 ± 0.08, H 14.46 ± 0.14 K 13.45 ± 0.10 [97b]
				Glob. spin-down → MJD →	$\sim 4E-11$ [98] 54101–57387					
9	XTE J1859+083	18:59:01.57	08:14:44.20	$9.79156 \pm 1E-5$ (2021) [98a]		$60.65 \pm 0.08$ [98b]	...	...	6.1–8.7 [98a]	...
				Loc. spin-up → MJD →	$\sim 1.53E-9$ [78] 57048–57149					Be [98a]
10	Swift J0243.6+6124	02:43:40.43	61:26:03.76	$9.8661 \pm 3E-4$ (2017) [98c]		$28.3 \pm 0.2$ [98d]	6E33–2E39 0.1–10 [98e, 98f]	...	5.5 ± 0.4 [98g]	...
				Loc. spin-up → MJD →	$\sim 2.14E-8$ [98d] 58027–58084					O9.5Ve [98h] B 13.83 ± 0.03, V 12.86 ± 0.01 R 12.18 ± 0.01, I 11.45 ± 0.02 [98h]
				Glob. spin-down → MJD →	$\sim 1.94E-10$ [78] 58161–58468					J 10.589 ± 0.023, H 10.208 ± 0.021 K 9.961 ± 0.018 [13a] $E(B - V) 1.24 \pm 0.02$ [98h]
11	IGR J17544-2619	17:54:25.27	-26:19:52.58	$11.58 \pm 0.03$ (2015) [99]		$4.926 \pm 0.001$ [100]	(0.2–5.3)E36 1–10 [2]	1.45 ± 0.03 [101]	3 ± 0.2 [2]	...
										O9 Ib [102] B 14.62 ± 0.05, V 12.89 ± 0.05

**Table 3**  
(Continued)

No.	Name	Eq. Coord. J2000		$P_s$ (s) Spin and Its Evol.	$\dot{P}$ (s s $^{-1}$ ) MJD	$P_{\text{orb}}$ (days)	$L_x$ (erg s $^{-1}$ ) Range (keV)	$B_{\text{ns}}$ ( $\times 10^{12}$ G)	dist (kpc)	Comp. Name Spec. Class and Photom.
		R.A.	Decl.							
12	IGR J18179-1621	18:17:52.18	-16:21:31.68	$11.8268 \pm 1E-4$ (2020) [102b]		...	<1E37 1.5–50 [102c]	~1.7 [103]	< 8 [102c]	$R 11.76 \pm 0.05, I$ $10.39 \pm 0.05$ [102a] $J 8.791 \pm 0.021, H 8.310 \pm 0.031$ $K 8.018 \pm 0.026$ [13a]
13	GS 0834-430	08:35:54.00	-43:11:17.50	$12.294 \pm 0.034$ (2012) [104] Loc. spin-up → MJD →	$105.8 \pm 0.4$ [105] $(-1.66 \pm 0.45)E-9$ [104] 56106–56110		$(0.1–5.5)E35$ 0.1–2.4 [106]	...	5 [106]	O–B [103] $H 16 \pm 0.1, K 13.14 \pm 0.04$ [103]
14	IGR J19294+1816	19:29:55.91	18:18:38.25	$12.485065 \pm 15E-6$ (2019) [107] Loc. spin-up → MJD → Glob. spin-down → MJD →		$116.93 \pm 0.05$ [108]	$(0.067–3.4)E36$ 3–79 [109]	~5 [109]	$11 \pm 1$ [109a]	...
15	Swift J1626.6-5156	16:26:36.52	-51:56:30.60	$15.3714 \pm 3E-4$ (2005) [110] Glob. spin-up → MJD →		$132.89 \pm 0.03$ [113]	$\sim 3.4E35$ 2–60 [112]	~0.86 [112]	$10.7 \pm 3.5$ [113]	...
16	XTE J1946+274	19:45:39.36	27:21:55.50	$15.757119 \pm 86E-6$ (2021) [114] Loc. spin-up → MJD →		$169.2 \pm 0.9$ [115]	$(0.5–5)E37$ 3–60 [117]	$3.1 \pm 0.1$ [117]	$7 \pm 2$ [62a]	$B0$ Ve [113] $B 16.81, V 15.54$ $R 15.81, I 14.27$ [113] $J 13.436 \pm 0.024, H 12.948 \pm 0.025$ $K 12.537 \pm 0.023$ [13a]
17	2S 1417-624	14:21:12.80	-62:41:54.00	$17.544701 \pm 8E-6$ (1999) [118] Glob. spin-up → MJD →		$42.12 \pm 0.03$ [119]	$1.4E34–1.3E36$ 3–20 [120]	...	$7.4 \pm 3$ [16a]	...
18	KS 1947+300	19:49:35.48	30:12:31.78	$18.78896 \pm 7E-5$ (2013) [122] Glob. spin-down → MJD → Loc. spin-up → MJD →		$40.415 \pm 0.01$ [123]	$(0.17–1.7)E36$ 1–10 [2]	~1.1 [124]	$8 \pm 2$ [62a]	...
19	IGR J18483-0311	18:48:17.21	-03:10:16.87	$21.0526 \pm 5E-4$ (2007) [127]	...	$18.52 \pm 0.01$ [128]	$1.6E34–7.8E36$ 20–100 [127]	...	3–4 [128]	...
20	XTE J1543-568	15:44:01.90	-56:42:43.00	$27.12156 \pm 59E-4$ (2001) [129] Glob. spin-up → MJD →		$75.56 \pm 0.25$ [129]	$(2.1–3.3)E36$ 1–10 [2]	...	~10 [129]	...
21	GS 1843+00	18:45:36.84	00:51:47.44	$29.477 \pm 0.001$ (1997) [130] Loc. spin-up → MJD →		$50–60$ [130]	$3E37$ 0.3–100 [130]	...	$\geq 10$ [130a]	...

**Table 3**  
(Continued)

No.	Name	Eq. Coord. J2000		$P_s$ (s) Spin and Its Evol.	$\dot{P}$ (s s <sup>-1</sup> ) MJD	$P_{\text{orb}}$ (days)	$L_x$ (erg s <sup>-1</sup> ) Range (keV)	$B_{\text{ns}} (\times 10^{12} \text{ G})$	dist (kpc)	Comp. Name Spec. Class and Photom.
		R.A.	Decl.							
										R 18.80 ± 0.05, I 16.79 ± 0.05 [130a] J 13.790 ± 0.035, H 12.820 ± 0.035 K 12.179 ± 0.037 [13a] $E(B - V) \sim 2.8$ [130a]
22	RX J0812.4-3114	08:12:28.36	-31:14:52.14	$31.908 \pm 0.009$ (2018) [131]		$\sim 81.3$ [132]	$\sim 2.3E36$ 3–30 [132]	...	$6.76 \pm 1.2$ [131]	V572 Pup B0.5 V–III [50] B 13.03 ± 0.02, V 12.74 ± 0.03 R 12.44 ± 0.05 [51a] J 11.335 ± 0.022, H 11.126 ± 0.022 K 10.909 ± 0.023 [13a]
23	EXO 2030+375	20:32:15.27	37:38:14.84	$41.4106 \pm 1E-4$ (2013) [133] Loc. spin-up → MJD →	$(-3.11 \pm 0.01)E-8$ [134] 53948–53953	$46.0205 \pm 2E-4$ [134]	$(0.092\text{--}6.4)E37$ 1–10 [2]	$\sim 3.1$ [135]	$3 \pm 0.2$ [62a]	V2246 Cyg B0 Ve [136] B 22.16, V 19.41 R 17.32, I 15.18 [62a] J 12.050 ± 0.020, H 10.835 ± 0.018 K 10.074 ± 0.016 [13a] $E(B - V) 3 \pm 0.2$ [62a]
24	IGR J18219-1347	18:21:54.82	-13:47:26.70	$52.468 \pm 3E-4$ (2020) [136a]	—	$72.44 \pm 0.3$ [136b]	$(2\text{--}5)E36$ 3–79 [136a]	...	10–15 [136a]	...
										B0–2 [136a] J21.3 ± 0.4, H 18.62 ± 0.07 K 16.93 ± 0.03 [136a]
25	AX J1700.2-4220	17:00:25.24	-42:19:00.28	$54.22 \pm 0.03$ (2010) [137]		$44.12 \pm 0.04$ [138]	$\sim 1E36$ 2–50 [137]	...	1.7–2.6 [139]	HD 15295 B0.5 IVe [139] B 9.05, R 9.52 [139a] J 7.445 ± 0.027, H 7.093 ± 0.036 K 6.729 ± 0.016 [13a]
26	GS 2138+56 (Cep X-4)	21:39:30.69	56:59:10.42	$65.3529 \pm 17E-4$ (2018) [140] Loc. spin-up → MJD →	$(-1.06 \pm 0.08)E-8$ [145] 56813–56831	$23\text{--}143$ [141]	$(0.27\text{--}1.4)E36$ 2–10 [142]	$3.4 \pm 0.2$ [142]	$7.5 \pm 0.6$ [143]	V490 Cep B1–2 Ve [143] J 11.829 ± 0.024, H 11.414 ± 0.028 K 10.926 ± 0.020 [13a]
					Glob. spin-down → MJD →	$(1.92 \pm 0.04)E\text{--}10$ [141] 49163–50641				
27	XTE J1906+090	19:04:47.48	09:02:41.80	$89.66 \pm 0.03$ (2003) [145a]		$26\text{--}30$ [145b]	$(0.07\text{--}7)E36$ 2–10 [145a]	...	$\geq 10$ [145c]	— Be [145a] J 15.18 ± 0.07, H 14.17 ± 0.11 K 13.50 ± 0.06.
28	GRO J1008-57	10:09:46.96	-58:17:35.60	$93.283 \pm 0.001$ (2017) [146] Loc. spin-up → MJD →	$(-4.45 \pm 0.04)E\text{--}8$ [151] 56993–57032	$249.48 \pm 0.04$ [147]	$(0.56\text{--}9.8)E36$ 1–10 [2]	$\sim 7.8$ [146]	$9.7 \pm 0.8$ [150]	...
					Glob. spin-down → MJD →	$(4.75 \pm 1.04)E\text{--}10$ [152] 48988–55196				B0 III–Ve [150] B 16.74, V 15.08 R 13.77, I 12.68 [150] J 10.943 ± 0.024, H 10.272 ± 0.023 K 9.718 ± 0.021 [13a] $E(B - V) 1.96 \pm 0.03$ [150]
29	GS 1843-024	18:48:17.70	56:59:10.42	$94.7171 \pm 3E-4$ (2017) [153] Glob. spin-up →	$\sim 2.44E\text{--}9$ [154]	$242.18 \pm 0.01$ [154]	$\sim 1E34$ 0.3–10 [153]	...	10–15 [153],[154]	...
					MJD →	48362–50600				O–B (SG) [153] H17.82 ± 0.04, K 15.52 ± 0.03 [153]
					Glob. spin-down →	$\sim 2.16E\text{--}9$ [78]				
					MJD →	56154–58103				
30	3A 0726-260	07:28:53.58	-26:06:28.88	$103.145 \pm 0.001$ (2016) [155]		$34.548 \pm 0.01$ [155a]	$\sim 2.8E35$ 2–20 [156]	...	$7 \pm 0.5$ [150]	V441 Pup O8.5 Ve [150] B 12.12, V 11.61

**Table 3**  
(Continued)

No.	Name	Eq. Coord. J2000		$P_s$ (s) Spin and Its Evol.	$\dot{P}$ (s s <sup>-1</sup> ) MJD	$P_{\text{orb}}$ (days)	$L_x$ (erg s <sup>-1</sup> ) Range (keV)	$B_{\text{ns}}$ ( $\times 10^{12}$ G)	dist (kpc)	Comp. Name Spec. Class and Photom.
		R.A.	Decl.							
31	1A 0535+262	05:38:54.57	26:18:56.84	$103.24 \pm 0.02$ (2020) [157]		$110 \pm 0.5$ [158]	$(0.0099-1.5)\text{E}37$ 1–10 [2]	$\sim 4.3$ [159]	$2.1 \pm 0.5$ [62a]	R 11.12, I 10.88 [150] $J 10.366 \pm 0.029$ , H 10.093 $\pm 0.024$ K 9.832 $\pm 0.023$ [13a] $E(B-V) 0.83 \pm 0.03$ [150]
	Loc. spin-up →	$(-6.73 \pm 0.23)\text{E}-8$ [162]		MJD →	55161–55197					B 9.74, V 10.73
	Glob. spin-up →	$\sim 1.6\text{E}-9$ [163]		MJD →	42531–47624					R 10.28, I 9.76 [62a]
	Glob. spin-down →	$\sim 1.5\text{E}-9$ [164]		MJD →	49353–53735					$J 8.368 \pm 0.021$ , H 8.272 $\pm 0.026$ K 8.157 $\pm 0.027$ [13a] $E(B-V) 0.77 \pm 0.04$ [62a]
32	AX J1749.1-2733	17:49:06.79	-27:32:32.40	$131.95 \pm 0.24$ (2007) [164a]		$185.5 \pm 1.1$ [164b]	$(0.41-1.3)\text{E}37$ 1–10 [2]	-	$16 \pm 3.5$ [164c]	... B1–2 [164c] $J > 18.7$ , H 17.43 $\pm 0.14$ K 15.18 $\pm 0.03$ [164c]
33	Swift J1816.7-1613	18:16:42.66	-16:13:23.40	$143.6863 \pm 0.0002$ (2017) [164d]	-	$118.5 \pm 0.8$ [164e]	$(0.01-5.5)\text{E}36$ 3–79 [164d]	...	7–13 [164d]	... B0–2 e [164d] H 17.56 $\pm 0.1$ , K 14.85 $\pm 0.02$ [164d]
	Loc. spin-up →	$\sim 5.93\text{E}-7$ [164f]		MJD →	54554–54563					
34	AX J1820.51434	18:20:29.50	-14:34:24.00	$152.26 \pm 0.04$ (1998) [165]		$54 \pm 0.4$ [166]	$(1.7-3.8)\text{E}36$ 1–10 [2]	...	$8.2 \pm 3.5$ [44a]	... B0 III–V [166] $J 15.41$ , H 13.25 K 11.75 [166]
	spin-down →	$(3.0 \pm 0.14)\text{E}-9$ [166]		MJD →	?					
35	MXB 0656-072	06:58:17.29	-07:12:35.20	$160.4 \pm 0.4$ (2003) [167]		$\sim 101.2$ [168]	$\sim 6.6\text{E}36$ 2–10 [167]	$3.67 \pm 0.06$ [167]	$5.7 \pm 0.5$ [143]	O9.5 Ve [170] B 13.25 $\pm 0.02$ , V 12.25 $\pm 0.02$ R 11.63 $\pm 0.02$ , I 10.97 $\pm 0.02$ [170] J 9.664 $\pm 0.026$ , H 9.332 $\pm 0.025$ K 9.013 $\pm 0.024$ [13a]
	Loc. spin-up →	$(-1.12 \pm 0.04)\text{E}-7$ [167]		MJD →	52930–52971					
36	IGR J11435-6109	11:44:00.29	-61:07:36.48	$161.76 \pm 0.01$ (2004) [170a]		$52.46 \pm 0.06$ [172]	$(0.99-2.1)\text{E}36$ 1–10 [2]	...	$\sim 8.6$ [172a]	... B0 V–B2 III [172a] $J 13.003 \pm 0.022$ , H 12.338 $\pm 0.021$ K 11.852 $\pm 0.019$ [13a]
18	IGR J11215-5952	11:21:46.82	-59:51:47.97	$187 \pm 0.12$ (2017) [173]		$\sim 164.6$ [174]	$(0.86-5.1)\text{E}36$ 1–10 [2]	...	$7 \pm 1$ [176]	HD 306414 B0.5 Ia [176] B 10.69 $\pm 0.01$ , V 10.23 $\pm 0.01$ R 10.00 $\pm 0.01$ [51a] J 8.548 $\pm 0.030$ , H 8.340 $\pm 0.036$ K 8.185 $\pm 0.023$ [13a] $E(B-V) 0.7$ [176]
38	1H 1238-599	12:42:01.70	-60:12:06.00	$191.196 \pm 0.084$ (1976) [177]		...	...	...	...	...
39	GRO J2058+42	20:58:47.54	41:46:37.18	$194.2201 \pm 0.0016$ (2019) [179]		$55? 110?$ [180] [181]	$1\text{E}34-4.2\text{E}37$ 3–80 [179][182]	$1-2$ [182]	$9 \pm 2.5$ [62a]	... O9.5–B0 IV–Ve [62a] B 16.04, V 14.89 R 14.16, I 13.35 [62a] $J 11.740 \pm 0.022$ , H 11.282 $\pm 0.018$ K 10.930 $\pm 0.017$ [13a] $E(B-V) 1.37 \pm 0.03$ [62a]
	Loc. spin-up →	$(-9.52 \pm 0.08)\text{E}-7$ [180]		MJD →	49974–50020					
40	RX J0440.9+4431	04:40:59.33	44:31:49.26	$206.01 \pm 0.47$ (2011) [183]		$150 \pm 0.2$ [183]	$(0.04-7.1)\text{E}36$ [184]	$\sim 3.2$ 3–100	$2.2 \pm 0.5$ [62a]	LS V+44 17 B0.2 Ve [62a]

**Table 3**  
(Continued)

No.	Name	Eq. Coord. J2000		$P_s$ (s) Spin and Its Evol.	$\dot{P}$ ( $s s^{-1}$ ) MJD	$P_{\text{orb}}$ (days)	$L_x$ ( $\text{erg s}^{-1}$ ) Range (keV)	$B_{\text{ns}} (\times 10^{12} \text{ G})$	dist (kpc)	Comp. Name Spec. Class and Photom.
		R.A.	Decl.							
		Glob. spin-down →		(6.4 ± 1.3)E-9 [186]			[184]			B 11.42, V 10.73
		MJD →		51179–56292						R 10.28, I 9.76 [62a]
		Loc. spin-up →		(−1.11 ± 0.33)E-7 [186a]						J 9.500 ± 0.023, H 9.317 ± 0.030
		MJD →		55706–55714						K 9.182 ± 0.018 [13a]
										E(B − V) 0.91 ± 0.03 [62a]
41	Swift J1845.70037	18:45:54.62	−00:39:34.20	207.379 ± 0.002 (2019) [187]		...	~2.4E35 0.1–100 [187]	...	10? [187]	...
42	XTE J1858+034	18:58:36.00	03:26:09.00	218.382 ± 0.002 (2019) [187b]		~380 [188]	(0.17–1.5)E37 1–10 [2]	~5.2 [187b]	~6 [188]	...
		Loc. spin-up →		~4.40E-7 [188]						Be [203]
		MJD →		52761–52773						B 19.61 ± 0.02, V 18.00 ± 0.02
										R 16.95 ± 0.01, I 15.32 ± 0.02 [203]
43	AX J1749.2-2725	17:49:12.28	−27:25:37.40	220.38 ± 0.20 (1997) [187c]		...	~7E34 2–10 [164c]	...	11–16 [164c]	...
		Glob. spin-up →		~9E-9 [164c]						BI-3 [164c]
		MJD →		50814–54831						J 18.58 ± 0.21, H 16.57 ± 0.07
										K 14.95 ± 0.05 [164c]
44	IGR J16465-4507	16:46:35.26	−45:07:04.61	228 ± 6 (2004) [189]		30.243 ± 0.035 [190]	(2.1–4.9)E36 1–10 [2]	...	2.7 ± 0.5 [190a]	...
										BO.5–1 Ib [190b]
										B 16.85 ± 0.01, V 14.62 ± 0.01
										R 13.55 ± 0.01, I 12.45 ± 0.01
										J 10.53 ± 0.05, H 10.01 ± 0.06
										K 9.83 ± 0.07 [190b]
										E(B − V) 1.82 ± 0.02 [190b]
45	4U 1258-61 (GX 304-1)	13:01:17.10	−61:36:06.64	275 ± 0.02 (2017) [191]		132.189 ± 0.02 [192]	1E34–2.2E37 3–79 [193]	~4.7 [194]	1.9 ± 0.05 [143]	V850 Cen
		Loc. spin-down →		(2.39 ± 0.51)E-8 [195]						BO.7 V [143]
		MJD →		55563–55677						V 14.4 [143]
		Loc. spin-up →		(−2.45 ± 0.25)E-7 [195]						J 9.798 ± 0.022, H 9.297 ± 0.022
		MJD →		55811–55821						K 9.040 ± 0.021 [13a]
46	2S 1145-619	11:48:00.02	−62:12:24.90	292.274 ± 0.001 (1985) [196]		186.68 ± 0.05 [197]	(0.84–1.9)E35 1–10 [2]	...	3.1 ± 0.5 [197a]	HD 102567
										BO.2 III [197b]
										B 9.06, V 9.00 [28a]
										J 8.682 ± 0.028, H 8.562 ± 0.009
										K 8.395 ± 0.011 [197a]
										E(B − V) 0.29 ± 0.02 [197a]
47	1E 1145.1-6141	11:47:28.56	−61:57:13.43	296.653 ± 0.021 (2019) [198]		14.365 ± 0.002 [199]	(0.1–4.7)E37 1–10 [2]	...	8.2 ± 1.5 [200]	...
		Glob. spin-up →		~1.06E-9 [199]						B2 Iae [200]
		MJD →		42614–51570						B 14.55, V 13.10
										R 14.11 [200]
										J 9.607 ± 0.026, H 9.110 ± 0.022
										K 8.810 ± 0.021 [13a]
										E(B − V) 1.61 ± 0.02 [200]
48	SGR 0755-2933	07:55:32.00	−29:33:08.00	308.26 ± 0.02 (2020) [200a]		~260 [200a]	~1E34 3–80 [200a]	...	3.5 ± 0.2 [200a]	...
49	IGR J21343+4738	21:34:20.37	47:38:00.21	322.71 ± 0.04 (2020) [200c]		~34.26 [200c]	(0.5–1.5)E35 2–12 [201]	...	10 ± 2.5 [62a]	...
										B1 IV shell [62a]
										B 14.68, V 14.16
										R 13.80, I 13.42 [62a]
										J 12.939 ± 0.02, H 12.726 ± 0.023
										K 12.529 ± 0.027 [13a]
										E(B − V) 0.75 ± 0.03 [62a]
50	IGR J17200-3116	17:20:05.91	−31:16:59.60	327.878 ± 0.024 (2013) [201a]		...	(0.9–1.2)E35 1–10 [201a]	...	5–10 [201a]	...
										Be [201a]
										J 13.581 ± 0.056, H 12.334 ± 0.057

**Table 3**  
(Continued)

No.	Name	Eq. Coord. J2000		$P_s$ (s) Spin and Its Evol.	$\dot{P}$ (s s $^{-1}$ ) MJD	$P_{\text{orb}}$ (days)	$L_x$ (erg s $^{-1}$ ) Range (keV)	$B_{\text{ns}}$ ( $\times 10^{12}$ G)	dist (kpc)	Comp. Name Spec. Class and Photom.
		R.A.	Decl.							
										K 11.983 ± 0.043 [62a]
51	IGR J00370+6122	00:37:09.64	61:21:36.49	$346 \pm 6$ (2006) [202]		$15.6649 \pm 0.0014$ [202a]	$(0.4\text{--}3)\text{E}36$ 3–60 [202]	...	$3.4 \pm 0.3$ [202b]	BD +60 73 B0.5 II–III [203] $B 10.24 \pm 0.02$ , V $9.70 \pm 0.02$ R $9.36 \pm 0.02$ , I $8.91 \pm 0.03$ [203] J $8.389 \pm 0.024$ , H $8.265 \pm 0.046$ [203] K $8.166 \pm 0.020$ [13a] $E(B - V) 0.75$ [203]
52	SAX J2103.5+4545	21:03:35.71	45:45:05.56	$351.13 \pm 0.02$ (2013) [204]		$\sim 12.68$ [205]	$(0.75\text{--}8.4)\text{E}36$ 1–10 [2]	...	$6 \pm 1.5$ [62a]	...
				Loc. spin-up → MJD →	$\sim 2.9\text{E}{-}7$ [208] 55481–55496					B0 Ve [207] B 15.34, V 14.20
				Glob. spin-down → MJD →	$\sim 1.8\text{E}{-}9$ [208] 55927–57022					R 13.49, I 12.75 [62a] J $11.842 \pm 0.021$ , H $11.535 \pm 0.021$ K $11.362 \pm 0.023$ [13a] $E(B - V) 1.36 \pm 0.05$ [62a]
53	IGR J06074+2205	06:07:26.61	22:05:47.76	$373.226 \pm 0.013$ (2017) [208a]		–	$\sim 1.5\text{E}34$ 0.2–12 [208a]	...	$4.1 \pm 1$ [62a]	GSC 01325-01064 B0.5 Ve B 12.85, V 12.21 R $11.80$ , I $11.32$ [62a] J $10.49 \pm 0.021$ , H $10.19 \pm 0.022$ K $9.96 \pm 0.019$ [13a] $E(B - V) 0.86 \pm 0.03$ [62a]
54	1A 1118-615	11:20:57.17	-61:55:00.17	$407.77 \pm 0.08$ (2009) [209]		$24 \pm 0.4$ [210]	$(0.23\text{--}2.5)\text{E}37$ 3–30 [209]	$\sim 4.8$ [212]	$5 \pm 2$ [213]	WRAY 15-793 O9.5 Ve [213] B 13.06, V 12.12 [211] J $9.563 \pm 0.024$ , H $9.071 \pm 0.023$ K $8.587 \pm 0.019$ [13a]
				Loc. spin-up → MJD →	$(-4.6 \pm 0.02)\text{E}{-}7$ [212] 54841–54865					
				Glob. spin-down → MJD →	$\sim 1.49\text{E}{-}8$ [78] 54832–55561					
55	4U 1907+09	19:09:37.14	09:49:55.28	$442.92 \pm 0.03$ (2018) [215]		$8.380 \pm 0.002$ [216]	$(0.36\text{--}4.8)\text{E}36$ 1–10 [2]	2 [34]	$4.4 \pm 1.2$ [62a]	...
				Glob. spin-down → MJD	$(6.87 \pm 0.04)\text{E}{-}9$ 45576–51080					O8–9 Ia [217] B 19.41, V 16.35 R $14.40$ , I $12.53$ [62a] J $8.63$ , K $8.80$ [94] $E(B - V) 3.31 \pm 0.1$ [62a]
56	IGR J01583+6713	01:58:18.49	67:13:23.46	$469.2$ (2005) [219]	–	$216\text{--}561$ [219]	$(0.01\text{--}4.4)\text{E}35$ 20–100 [220]	$4 \pm 0.4$ [220]	$3.4 \pm 0.8$ [62a]	...
										B2 IVe [219] B 15.71, V 14.41 R $13.51$ , I $12.66$ [62a] J $11.481 \pm 0.026$ , H $11.03 \pm 0.03$ K $10.601 \pm 0.021$ [13a] $E(B - V) 1.44 \pm 0.04$ [62a]
57	MAXI J1409-619	14:08:02.56	-61:59:00.30	$506.93 \pm 0.05$ (2010) [221]		$14.7 \pm 0.4$ [221a]	$(0.07\text{--}2)\text{E}37$ 2–10 [222]	$\sim 3.8$ [223]	$\sim 14.5$ [223]	...
				Loc. spin-up → MJD →	$(-4.07 \pm 0.18)\text{E}{-}6$ [224] 55530–55546					B0 III–V [223] J $15.874 \pm 0.086$ , H $13.620 \pm 0.022$ K $12.560 \pm 0.021$ [223]
58	4U 1909+07	19:10:48.21	07:35:51.71	$603.6 \pm 0.1$ (2017) [224a]		$4.4 \pm 0.001$ [226]	$(0.35\text{--}3.5)\text{E}36$ 1–10 [2]	$\sim 3.8$ [225]	$7 \pm 3$ [227]	...
				Glob. spin-down → MJD →	$\sim 7.15\text{E}{-}9$ [228] 54280–55600					O7.5–O9.5 I [227] J $13.228 \pm 0.021$ , H $11.457 \pm 0.027$ K $10.480 \pm 0.022$ [227]
59	IGR J13020-6359	13:01:58.72	-63:58:08.83	$642.90 \pm 0.01$ (2014) [228a]		...	$(0.8\text{--}2.6)\text{E}35$ 3–79 [228a]	...	$4\text{--}7$ [230]	...
				Glob. spin-up → MJD →	$\sim 2\text{E}{-}7$ [229] 51910–53370					B0.5 Ve [231] J $12.962 \pm 1.339$ , H $12.047 \pm 0.031$ K $11.346 \pm 0.088$ [13a]

**Table 3**  
(Continued)

No.	Name	Eq. Coord. J2000		$P_s$ (s) Spin and Its Evol.	$\dot{P}$ (s s $^{-1}$ ) MJD	$P_{\text{orb}}$ (days)	$L_x$ (erg s $^{-1}$ ) Range (keV)	$B_{\text{ns}}$ ( $\times 10^{12}$ G)	dist (kpc)	Comp. Name Spec. Class and Photom.
		R.A.	Decl.							
60	IGR J18462-0223	18:46:12.79	-02:22:26.04	$997 \pm 1$ (2011) [233]		$\sim 2.13$ [234]	(0.011–2.2)E37 18–60 [234]	...	$\sim 11$ [234]	...
61	IGR J16418-4532	16:41:50.80	-45:32:25.37	$1212 \pm 6$ (2011) [235]	—	$3.7389 \pm 4\text{E-}4$ [236]	(0.3–2.1)E37 1–10 [2]	...	$\sim 13$ [235]	...
62	SAX J2239.3+6116	22:39:20.84	61:16:26.61	$1247.2 \pm 0.7$ (2001) [237]	...	$262.6 \pm 0.7$ [237]	2.3E36 2–28 [237]	...	$\sim 4.4$ [238]	...
										B0 V–B2 III [238] B 16.5, V 15.1 R 14.1 [238]
										J 11.450 $\pm 0.026$ , H 10.955 $\pm 0.031$ K 10.557 $\pm 0.021$ [13a] $E(B - V)$ 1.8 [238]
63	IGR J16320-4751	16:32:01.87	-47:52:28.30	$1309 \pm 40$ (2003) [239]	Glob, spin-up $\rightarrow$ MJD $\rightarrow$	$8.99 \pm 0.01$ [240] $\sim 8.57\text{E-}7$ [239] 50449–53735	(0.18–2.5)E36 1–10 [2]	...	$\sim 3.5$ [102]	...
64	AX J1910.7+0917	19:10:43.55	09:16:29.83	$36200 \pm 110$ (2011) [241]		...	(0.017–1)E36 1–10 [241]	...	$16.0 \pm 0.5$ [242]	...
										B (sg) [242]
										J $> 17.1$ , H $14.43 \pm 0.05$ K $13.135 \pm 0.003$ [242]

#### Note.

References for Table 3: (71) Cusumano et al. (2000); (72) Kaaret et al. (2000); (73) Kaaret et al. (1999); (74) Mereghetti & La Palombara (2009); (75) Belczynski & Ziołkowski (2009); (76) Hemphill et al. (2019a); (77) Galloway et al. (2005); (78) Malacaria et al. (2020); (79) Strader et al. (2019); (80) Ding et al. (2021); (81) Boldin et al. (2013); (82) Nagase et al. (1991); (83) Negueruela & Okazaki (2001); (84) Li et al. (2012a); (86) Zhang et al. (2005); (87) Makishima et al. (1990); (88) Negueruela et al. (1999); (90) Devaraj & Paul (2022); (91) Scott et al. (1997); (91a) Lutovinov et al. (2019); (92) Shaw et al. (2009); (93) Bamba et al. (2001); (94) Nespoli et al. (2008); (95) Shtykovsky et al. (2019); (95a) Corbet et al. (2022); (96) Halpern & Gotthelf (2007); (96a) UKIDSS Consortium (2012); (97) Christodoulou et al. (2022); (97a) Malacaria et al. (2022); (97b) Lutovinov et al. (2016); (97c) Pahari & Pal (2012); (98) Tsygankov et al. (2016); (98a) Salganik et al. (2022); (98b) Corbet (2009); (98c) Jenke & Wilson-Hodge (2017); (98d) Doroshenko et al. (2018); (98e) Doroshenko et al. (2020b); (98f) Wilson-Hodge et al. (2018); (98g) GAIA Collaboration (2022); (98h) Reig et al. (2020); (99) Romano et al. (2015); (100) Clark et al. (2009); (101) Bhalerao et al. (2015); (102) Rahoui et al. (2008); (102a) Bozzo et al. (2016); (102b) Esposito et al. (2020); (102c) Li et al. (2012b); (103) Nowak et al. (2012); (104) Jenke et al. (2012b); (105) Wilson et al. (1997); (106) Israel et al. (2000); (107) Raman et al. (2021); (108) Corbet & Krimm (2009); (109) Tsygankov et al. (2019a); (109a) Rodes-Roca et al. (2018); (109b) Fermi Collaboration (2021g); IGR J19294+1816; (110) Reig et al. (2008); (111) Baykal & Göğüş (2010); (112) DeCesar et al. (2013); (113) Reig et al. (2011); (114) Dee Chandra et al. (2023); (115) Wilson et al. (2003); (116) Müller et al. (2012); (117) Marcu-Cheatham et al. (2015); (118) Raichur & Paul (2010); (119) Finger et al. (1996); (120) İnam et al. (2004); (121) Negueruela (1998); (121a) Grindlay et al. (1984); (122) Ballhausen et al. (2016); (123) Galloway et al. (2004); (124) Fürst et al. (2014b); (125) Negueruela et al. (2003); (126) Fermi Collaboration (2021h); KS 1947+300; (127) Sguera et al. (2007); (128) Rahoui & Chaty (2008); (129) in't Zand et al. (2001a); (130) Piraino et al. (2000); (130a) Israel et al. (2001); (131) Zhao et al. (2019); (132) Corbet & Peele (2000); (133) Naik et al. (2013); (134) Wilson et al. (2008); (135) Reig & Coe (1999); (136) Reig et al. (2014a); (136a) O'Connor et al. (2022); (136b) La Parola et al. (2013); (137) Markwardt et al. (2010); (138) Corbet et al. (2010b); (139) Negueruela & Schurch (2007); (139a) Anderson et al. (2014); (140) Mukerjee & Antia (2021); (141) Wilson et al. (1999); (142) McBride et al. (2007); (143) Reig & Fabbregat (2022); (145) Fermi Collaboration (2021d); Cep X-4); (145a) Göğüş et al. (2005); (145b) Wilson et al. (2002); (145c) Marsden et al. (1998); (146) Ge et al. (2020); (147) Kühnel et al. (2013); (150) Riquelme et al. (2012); (151) Fermi Collaboration (2021e); GRO J1008-57; (152) Wang (2014); (153) Nabizadeh et al. (2022); (154) Finger et al. (1999); (155) Roy et al. (2020); (155a) Corbet et al. (2016); (156) Corbet & Peele (1997); (157) Coley et al. (2023); (158) Coe et al. (2006); (159) Kendziorra et al. (1994); (161) Giangrande et al. (1980); (162) Fermi Collaboration (2021a); 1A 0535+262; (163) Coe et al. (1990); (164) Hill et al. (2007); (164a) Karasev et al. (2008); (164b) Zurita Heras & Chaty (2008); (164c) Karasev et al. (2010); (164d) Nabizadeh et al. (2019b); (164e) La Parola et al. (2014); (164f) Krimm et al. (2013); (165) Kinugasa et al. (1998); (166) Segreto et al. (2013); (167) McBride et al. (2006); (168) Yan et al. (2012); (170) Nespoli et al. (2012); (170a) in't Zand & Heise (2004); (171) Torrejón & Negueruela (2007); (172) Corbet & Remillard (2005); (172a) Masetti et al. (2009); (173) Sidoli et al. (2020); (174) Romano et al. (2009); (176) Lorenzo et al. (2014); (177) Huckle et al. (1977); (179) Mukerjee et al. (2020); (180) Wilson et al. (1998); (181) Bildsten et al. (1997); (182) Molkov et al. (2019); (183) Ferrigno et al. (2013); (184) Tsygankov et al. (2012); (185) Reig et al. (2005a); (186) La Palombara et al. (2012); (186a) Fermi Collaboration (2021k); RX J0440.9+4431; (187) Doroshenko et al. (2020a); (187a) McCollum & Laine (2019); (187b) Tsygankov et al. (2021); (187c) Torii et al. (1998); (188) Doroshenko et al. (2008); (189) Lutovinov et al. (2005a); (190) La Parola et al. (2010); (190a) Arnason et al. (2021); (190b) Chaty et al. (2016); (191) Rouco Escorial et al. (2018); (192) Sugizaki et al. (2015); (193) Tsygankov et al. (2019b); (194) Yamamoto et al. (2011); (195) Postnov et al. (2015); (196) Cook & Warwick (1987); (197) Wilson-Hodge (1999); (197a) Stevens et al. (1997); (197b) Alfonso-Garzón et al. (2017); (198) Ghising et al. (2022); (199) Ray & Chakrabarty (2002); (200) Densham & Charles (1982); (200a) Doroshenko et al. (2021); (200b) Chrimis et al. (2022); (200c) Gorban et al. (2022); (201) Reig & Zezas (2014); (201a) Esposito et al. (2014); (202) in't Zand et al. (2007); (202a) Uchida et al. (2021); (202b) Hainich et al. (2020); (203) Reig et al. (2005b); (204) Reig et al. (2014b); (205) Baykal et al. (2002); (207) Reig et al. (2004); (208) Camero et al. (2014); (208a) Reig & Zezas (2018); (209) Nespoli & Reig (2011); (210) Staubert et al. (2011); (211) Reed (2003); (212) Doroshenko et al. (2010); (213) Janot-Pacheco et al. (1981); (215) Tobrey et al. (2023); (216) Marshall & Ricketts (1980); (217) Cox et al. (2005); (218) Baykal et al. (2001); (219) Kaur et al. (2008); (220) Wang (2010); (221) Camero-Arranz et al. (2010); (221a) Dönmez et al. (2020); (222) Kaur et al. (2010a); (223) Orlandini et al. (2012); (224) Fermi Collaboration (2021i); MAXI J1409-619; (224a) Jaisawal et al. (2020); (225) Jaisawal et al. (2013); (226) Wen et al. (2000); (227) Morel & Grosdidier (2005); (228) Şahiner et al. (2012); (228a) Krivonos et al. (2015); (229) Chernyakova et al. (2005); (230) Chernyakova et al. (2006); (231) Coleiro et al. (2013); (233) Bodaghee et al. (2012a); (234) Sguera et al. (2013); (235) Sidoli et al. (2012); (236) Corbet et al. (2006); (237) in't Zand et al. (2001b); (238) in't Zand et al. (2000); (239) Lutovinov et al. (2005b); (240) García et al. (2018); (241) Sidoli et al. (2017); (242) Rodes-Roca et al. (2013).

(This table is available in machine-readable form.)

## ORCID iDs

- Vitaliy Kim <https://orcid.org/0000-0003-1202-9751>  
 Il'dana Izmailova <https://orcid.org/0000-0001-9878-0989>  
 Yerlan Aimuratov <https://orcid.org/0000-0001-5717-6523>

## References

- Alfonso-Garzón, J., Domingo, A., Mas-Hesse, J. M., & Giménez, A. 2012, *A&A*, **548**, A79  
 Alfonso-Garzón, J., Fabregat, J., Reig, P., et al. 2017, *A&A*, **607**, A52  
 Anderson, G. E., Gaensler, B. M., Kaplan, D. L., et al. 2014, *ApJS*, **212**, 13  
 Angelini, L., Church, M. J., Parmar, A. N., Balucinska-Church, M., Mineo, T., et al. 1998, *A&A*, **339**, L41  
 Arnason, R. M., Papei, H., Barnby, P., Bahramian, A., Gorski, M. D., et al. 2021, *MNRAS*, **502**, 5455  
 Arons, J., & Lea, S. M. 1976, *ApJ*, **210**, 792  
 Astropy Collaboration, Price-Whelan, A. M., Lim, P. L., et al. 2022, *ApJ*, **935**, 167  
 Astropy Collaboration, Price-Whelan, A. M., Sipőcz, B. M., et al. 2018, *AJ*, **156**, 123  
 Astropy Collaboration, Robitaille, T. P., Tollerud, E. J., et al. 2013, *A&A*, **558**, A33  
 Ballhausen, R., Kühnel, M., Pottschmidt, K., et al. 2016, *A&A*, **591**, A65  
 Bamba, A., Yokogawa, J., Ueno, M., Koyama, K., & Yamauchi, S. 2001, *PASJ*, **53**, 1179  
 Barnstedt, J., Staubert, R., Santangelo, A., et al. 2008, *A&A*, **486**, 293  
 Barthelmy, S. D., D'Elia, V., Gehrels, N., et al. 2016, GCN, **19204**, 1  
 Baykal, A., Inam, Ç., Ali Alpar, M., in't Zand, J., & Strohmayer, T. 2001, *MNRAS*, **327**, 1269  
 Baykal, A., Göğüş, E., Çağdaş İnam, S., & Belloni, T. 2010, *ApJ*, **711**, 1306  
 Baykal, A., Stark, M. J., & Swank, J. H. 2002, *ApJ*, **569**, 903  
 Belczynski, K., & Ziolkowski, J. 2009, *ApJ*, **707**, 870  
 Bhalerao, V., Romano, P., Tomsick, J., et al. 2015, *MNRAS*, **447**, 2274  
 Bildsten, L., Chakrabarty, D., Chiò, J., et al. 1997, *ApJS*, **113**, 367  
 Bird, A. J., Bazzano, A., Malizia, A., et al. 2016, *ApJS*, **223**, 15  
 Bodaghee, A., Courvoisier, T. J. L., Rodriguez, J., et al. 2007, *A&A*, **467**, 585  
 Bodaghee, A., Tomsick, J. A., Fornasini, F. M., et al. 2016, *ApJ*, **823**, 146  
 Bodaghee, A., Tomsick, J. A., & Rodriguez, J. 2012a, *ApJ*, **753**, 3  
 Bodaghee, A., Tomsick, J. A., Rodriguez, J., & James, J. B. 2012b, *ApJ*, **744**, 108  
 Bodaghee, A., Walter, R., Zurita Heras, J. A., et al. 2006, *A&A*, **447**, 1027  
 Boldin, P. A., Tsygankov, S. S., & Lutovinov, A. A. 2013, *AstL*, **39**, 375  
 Bonning, E. W., & Falanga, M. 2005, *A&A*, **436**, L31  
 Bozzo, E., Bhalerao, V., Pradhan, P., et al. 2016, *A&A*, **596**, A16  
 Bradt, H. V. D., & McClintock, J. E. 1983, *ARA&A*, **21**, 13  
 Camero, A., Zurita, C., Gutiérrez-Soto, J., et al. 2014, *A&A*, **568**, A115  
 Camero-Arranz, A., Finger, M. H., & Jenke, P. 2010, ATel, **3069**, 1  
 CGRO Collaboration 2000, The Burst And Transient Source Experiment (BATSE) Database, <https://heasarc.gsfc.nasa.gov/FTP/compton/data/batse/pulsar/histories/>  
 Chakrabarty, D., Wang, Z., Lee, J., & Roche, P. 2002, *ApJ*, **573**, 789  
 Chaty, S. 2008, ChJAS, **8**, 197  
 Chaty, S. 2022, Accreting Binaries; Nature, Formation, and Evolution (Bristol: IOP Publishing)  
 Chaty, S., LeReun, A., Negueruela, I., et al. 2016, *A&A*, **591**, A87  
 Chernyakova, M., Lutovinov, A., Rodríguez, J., & Revnivtsev, M. 2005, *MNRAS*, **364**, 455  
 Chernyakova, M., Lutovinov, A., Rodríguez, J., & Revnivtsev, M. 2006, in Populations of High Energy Sources in Galaxies, ed. E. J. A. Meurs & G. Fabbiano, Vol. 230 (Cambridge: Cambridge Univ. Press), 33  
 Chrimes, A. A., Levan, A. J., Fruchter, A. S., et al. 2022, *MNRAS*, **512**, 6093  
 Christodoulou, D. M., Bhattacharya, S., Laycock, S. G. T., & Kazanas, D. 2022, *ApJ*, **929**, 137  
 Clark, D. J., Hill, A. B., Bird, A. J., et al. 2009, *MNRAS*, **399**, L113  
 Coburn, W., Heindl, W. A., Rothschild, R. E., et al. 2002, *ApJ*, **580**, 394  
 Coe, M. J., Carstairs, I. R., Court, A. J., et al. 1990, *MNRAS*, **243**, 475  
 Coe, M. J., Reig, P., McBride, V. A., Galache, J. L., & Fabregat, J. 2006, *MNRAS*, **368**, 447  
 Coleiro, A., & Chaty, S. 2013, *ApJ*, **764**, 185  
 Coleiro, A., Chaty, S., Zurita Heras, J. A., Rahoui, F., & Tomsick, J. A. 2013, *A&A*, **560**, A108  
 Coley, J., Jaiswal, G. K., Arzoumanian, Z., et al. 2023, AAS Meeting, **55**, 428.07  
 Coley, J. B., Corbet, R. H. D., Fürst, F., et al. 2019, *ApJ*, **879**, 34  
 Cook, M. C., & Warwick, R. S. 1987, *MNRAS*, **225**, 369  
 Corbet, R., Barbier, L., Barthelmy, S., et al. 2006, ATel, **779**, 1  
 Corbet, R. H. D., Barthelmy, S. D., Baumgartner, W. H., et al. 2010a, ATel, **2598**, 1  
 Corbet, R. H. D., Coley, J. B., Gendreau, K. C., et al. 2022, ATel, **15614**, 1  
 Corbet, R. H. D., Coley, J. B., & Krimm, H. A. 2016, ATel, **9823**, 1  
 Corbet, R. H. D., Coley, J. B., & Krimm, H. A. 2017, *ApJ*, **846**, 161  
 Corbet, R. H. D., in't Zand, J. J. M., Levine, A. M., & Marshall, F. E. 2009, *ApJ*, **695**, 30  
 Corbet, R. H. D., & Krimm, H. A. 2009, ATel, **2008**, 1  
 Corbet, R. H. D., & Krimm, H. A. 2013, *ApJL*, **778**, 45  
 Corbet, R. H. D., Krimm, H. A., & Skinner, G. K. 2010b, ATel, **2559**, 1  
 Corbet, R. H. D., Markwardt, C. B., & Tueller, J. 2007, *ApJ*, **655**, 458  
 Corbet, R. H. D., Marshall, F. E., Peele, A. G., & Takeshima, T. 1999, *ApJ*, **517**, 956  
 Corbet, R. H. D., & Mukai, K. 2002, *ApJ*, **577**, 923  
 Corbet, R. H. D., & Peele, A. G. 1997, *ApJL*, **489**, L83  
 Corbet, R. H. D., & Peele, A. G. 2000, *ApJL*, **530**, L33  
 Corbet, R. H. D., & Remillard, R. 2005, ATel, **377**, 1  
 Cox, N. L. J., Kaper, L., & Mokiem, M. R. 2005, *A&A*, **436**, 661  
 Cusumano, G., Maccarone, M. C., Nicastro, L., Sacco, B., & Kaaret, P. 2000, *ApJL*, **528**, L25  
 Cusumano, G., Segreto, A., La Parola, V., et al. 2013, *MNRAS*, **436**, L74  
 Cutri, R. M., Skrutskie, M. F., van Dyk, S., et al. 2003, yCat, **2246**, 0  
 D'Aì, A., Cusumano, G., LaParola, V., et al. 2011, *A&A*, **532**, A73  
 D'Amico, F., Jablonski, F., Rodrigues, C. V., Cieslinski, D., & Hickel, G. 2006, in AIP Conf. Proc. 840, The Transient Milky Way: A Perspective for MIRAX, ed. F. D'Amico, J. Braga, & R. E. Rothschild (Melville, NY: AIP), 97  
 Davidson, K., & Ostriker, J. P. 1973, *ApJ*, **179**, 585  
 de Burgos, A., Simón-Díaz, S., Urbaneja, M. A., & Negueruela, I. 2023, *A&A*, **674**, A212  
 DeCesar, M. E., Boyd, P. T., Pottschmidt, K., et al. 2013, *ApJ*, **762**, 61  
 Delgado-Martí, H., Levine, A. M., Pfahl, E., & Rappaport, S. A. 2001, *ApJ*, **546**, 455  
 Densham, R. H., & Charles, P. A. 1982, *MNRAS*, **201**, 171  
 Deo Chandra, A., Roy, J., & Agrawal, P. C. 2023, *RAA*, **23**, 045003  
 Devaraj, A., & Paul, B. 2022, *MNRAS*, **514**, L46  
 Ding, Y. Z., Wang, W., Zhang, P., et al. 2021, *MNRAS*, **503**, 6045  
 Di Salvo, T., Burderi, L., Robba, N. R., & Guainazzi, M. 1998, *ApJ*, **509**, 897  
 Dönmez, Ç. K., Serim, M. M., İnam, S. Ç., et al. 2020, *MNRAS*, **496**, 1768  
 Doroshenko, V., Santangelo, A., Tsygankov, S. S., & Ji, L. 2021, *A&A*, **647**, A165  
 Doroshenko, V., Suchý, S., Santangelo, A., et al. 2010, *A&A*, **515**, L1  
 Doroshenko, V., Tsygankov, S., Long, J., et al. 2020a, *A&A*, **634**, A89  
 Doroshenko, V., Tsygankov, S., & Santangelo, A. 2018, *A&A*, **613**, A19  
 Doroshenko, V., Zhang, S. N., Santangelo, A., et al. 2020b, *MNRAS*, **491**, 1857  
 Doroshenko, V. A., Doroshenko, R. F., Postnov, K. A., Cherepashchuk, A. M., & Tsygankov, S. S. 2008, *ARep*, **52**, 138  
 Ducati, J. R. 2002, yCat, **2237**, 0  
 Esposito, P., Israel, G., Sidoli, L., et al. 2013, *MNRAS*, **433**, 2028  
 Esposito, P., Israel, G. L., Rea, N., Borghese, A., & Coti Zelati, F. 2020, ATel, **13625**, 1  
 Esposito, P., Israel, G. L., Sidoli, L., et al. 2014, *MNRAS*, **441**, 1126  
 Falanga, M., Bozzo, E., Lutovinov, A., et al. 2015, *A&A*, **577**, A130  
 Fermi Collaboration 2022, GBM Accreting Pulsar Histories, <https://gamma-ray.nsstc.nasa.gov/gbm/science/pulsars.html>  
 Fermi Collaboration 2021a, Fermi GBM Accreting Pulsar Histories (IA 0535 +262), <https://gamma-ray.nsstc.nasa.gov/gbm/science/pulsars/lightcurves/a0535.html>  
 Fermi Collaboration 2021b, Fermi GBM Accreting Pulsar Histories (4U 1538-52), <https://gamma-ray.nsstc.nasa.gov/gbm/science/pulsars/lightcurves/4u1538.html>  
 Fermi Collaboration 2021c, Fermi GBM Accreting Pulsar Histories (Cen X-3), <https://gamma-ray.nsstc.nasa.gov/gbm/science/pulsars/lightcurves/cenx3.html>  
 Fermi Collaboration 2021d, Fermi GBM Accreting Pulsar Histories (Cep X-4), <https://gamma-ray.nsstc.nasa.gov/gbm/science/pulsars/lightcurves/cep4.html>  
 Fermi Collaboration 2021e, Fermi GBM Accreting Pulsar Histories (GRO J1008-57), <https://gamma-ray.nsstc.nasa.gov/gbm/science/pulsars/lightcurves/groj1008.html>  
 Fermi Collaboration 2021f, Fermi GBM Accreting Pulsar Histories (GX 301-2), <https://gamma-ray.nsstc.nasa.gov/gbm/science/pulsars/lightcurves/gx301m2.html>

- Fermi Collaboration 2021g, Fermi GBM Accreting Pulsar Histories (IGR J19294+1816), <https://gamma-ray.msfc.nasa.gov/gbm/science/pulsars/lightcurves/igrj19294.html>
- Fermi Collaboration 2021h, Fermi GBM Accreting Pulsar Histories (KS 1947 +300), <https://gamma-ray.msfc.nasa.gov/gbm/science/pulsars/lightcurves/ks1947.html>
- Fermi Collaboration 2021i, Fermi GBM Accreting Pulsar Histories (MAXI J1409-619), <https://gamma-ray.msfc.nasa.gov/gbm/science/pulsars/lightcurves/maxij1409.html>
- Fermi Collaboration 2021j, Fermi GBM Accreting Pulsar Histories (OAO 1657-415), <http://gamma-ray.msfc.nasa.gov/gbm/science/pulsars/lightcurves/oao1657.fits.gz>
- Fermi Collaboration 2021k, Fermi GBM Accreting Pulsar Histories (RX J0440.9+4431), <https://gamma-ray.msfc.nasa.gov/gbm/science/pulsars/lightcurves/rxj0440.html>
- Fermi Collaboration 2021, Fermi GBM Accreting Pulsar Histories (Vela X-1), <https://gamma-ray.msfc.nasa.gov/gbm/science/pulsars/lightcurves/velax1.html>
- Ferrigno, C., Farinelli, R., Bozzo, E., et al. 2013, *A&A*, **553**, A103
- Finger, M. H., Bildsten, L., Chakrabarty, D., et al. 1999, *ApJ*, **517**, 449
- Finger, M. H., Ikhsanov, N. R., Wilson-Hodge, C. A., & Patel, S. K. 2010, *ApJ*, **709**, 1249
- Finger, M. H., Wilson, R. B., & Chakrabarty, D. 1996, *A&AS*, **120**, 209
- Fortin, F., García, F., Simaz Bunzel, A., & Chaty, S. 2023, *A&A*, **671**, A149
- Fürst, F., Pottschmidt, K., Wilms, J., et al. 2014a, *ApJ*, **780**, 133
- Fürst, F., Pottschmidt, K., Wilms, J., et al. 2014b, *ApJL*, **784**, L40
- GAIA Collaboration 2022, GAIA DR3 Catalog, <https://www.cosmos.esa.int/web/gaia/data-release-3>
- Galloway, D. K., Morgan, E. H., & Levine, A. M. 2004, *ApJ*, **613**, 1164
- Galloway, D. K., Wang, Z., & Morgan, E. H. 2005, *ApJ*, **635**, 1217
- García, F., Fogantini, F. A., Chaty, S., & Combi, J. A. 2018, *A&A*, **618**, A61
- Ge, M. Y., Ji, L., Zhang, S. N., et al. 2020, *ApJL*, **899**, L19
- Ghising, M., Tobrej, M., Rai, B., Tamang, R., & Paul, B. C. 2022, *MNRAS*, **517**, 4132
- Ghosh, P., & Lamb, F. K. 1979a, *ApJ*, **232**, 259
- Ghosh, P., & Lamb, F. K. 1979b, *ApJ*, **234**, 296
- Giangrande, A., Giovannelli, F., Bartolini, C., Guarneri, A., & Piccioni, A. 1980, *A&AS*, **40**, 289
- Gnedin, I. N., & Sunyaev, R. A. 1974, *A&A*, **36**, 379
- Göğüş, E., Patel, S. K., Wilson, C. A., et al. 2005, *ApJ*, **632**, 1069
- Gorban, A. S., Molkov, S. V., Lutovinov, A. A., & Semena, A. N. 2022, *AstL*, **48**, 798
- Grindlay, J. E., Petro, L. D., & McClintock, J. E. 1984, *ApJ*, **276**, 621
- Hainich, R., Oskinova, L. M., Torrejón, J. M., et al. 2020, *A&A*, **634**, A49
- Halpern, J. P., & Gotthelf, E. V. 2007, *ApJ*, **669**, 579
- Harris, C. R., Millman, K. J., van der Walt, S. J., et al. 2020, *Natur*, **585**, 357
- Hemphill, P., Coley, J., Fuerst, F., et al. 2019a, *ATel*, **12556**, 1
- Hemphill, P. B., Rothschild, R. E., Caballero, I., et al. 2013, *ApJ*, **777**, 61
- Hemphill, P. B., Rothschild, R. E., Cheatham, D. M., et al. 2019b, *ApJ*, **873**, 62
- Hill, A. B., Bird, A. J., Dean, A. J., et al. 2007, *MNRAS*, **381**, 1275
- Hill, A. B., Walter, R., Knigge, C., et al. 2005, *A&A*, **439**, 255
- Høg, E., Fabricius, C., Makarov, V. V., et al. 2000, *A&A*, **355**, L27
- Houk, N. 1978, Michigan Catalogue of Two-dimensional Spectral Types for the HD Stars (Ann Arbor, MI: Univ. Michigan)
- Huckle, H. E., Mason, K. O., White, N. E., et al. 1977, *MNRAS*, **180**, 21P
- Hunter, J. D. 2007, *CSE*, **9**, 90
- Hutchings, J., Crampton, D., van Paradijs, J., & White, N. 1979, *ApJ*, **229**, 1079
- Ikhsanov, N. R., & Finger, M. H. 2012, *ApJ*, **753**, 1
- Ikhsanov, N. R., Likh, Y. S., & Beskrovnaia, N. G. 2014, *ARep*, **58**, 376
- Ikhsanov, N. R., & Mereghetti, S. 2015, *MNRAS*, **454**, 3760
- İnam, S. Ç., Baykal, A., Matthew Scott, D., Finger, M., & Swank, J. 2004, *MNRAS*, **349**, 173
- in't Zand, J., & Heise, J. 2004, *ATel*, **362**, 1
- in't Zand, J. J. M., Corbet, R. H. D., & Marshall, F. E. 2001a, *ApJL*, **553**, L165
- in't Zand, J. J. M., Halpern, J., Eracleous, M., et al. 2000, *A&A*, **361**, 85
- in't Zand, J. J. M., Kuiper, L., den Hartog, P. R., Hermans, W., & Corbet, R. H. D. 2007, *A&A*, **469**, 1063
- in't Zand, J. J. M., Swank, J., Corbet, R. H. D., & Markwardt, C. B. 2001b, *A&A*, **380**, L26
- Integral Collaboration 2022, INTEGRAL Data Archives, <https://www.cosmos.esa.int/web/integral/integral-data-archives>
- Islam, N., Maitra, C., Pradhan, P., & Paul, B. 2015, *MNRAS*, **446**, 4148
- Israel, G. L., Belfiore, A., Stella, L., et al. 2017, *Sci*, **355**, 817
- Israel, G. L., Covino, S., Campana, S., et al. 2000, *MNRAS*, **314**, 87
- Israel, G. L., Negueruela, I., Campana, S., et al. 2001, *A&A*, **371**, 1018
- Jaisawal, G. K., Naik, S., Ho, W. C. G., et al. 2020, *MNRAS*, **498**, 4830
- Jaisawal, G. K., Naik, S., & Paul, B. 2013, *ApJ*, **779**, 54
- Janot-Pacheco, E., Illovaisky, S. A., & Chevalier, C. 1981, *A&A*, **99**, 274
- Jenke, P., Finger, M., Wilson-Hodge, C., & Camero-Arranz, A. 2012a, *ApJ*, **759**, 124
- Jenke, P., Finger, M. H., & Connaughton, V. 2012b, *ATel*, **4235**, 1
- Jenke, P., & Wilson-Hodge, C. A. 2017, *ATel*, **10812**, 1
- Kaaret, P., Cusumano, G., & Sacco, B. 2000, *ApJL*, **542**, L41
- Kaaret, P., Piraino, S., Halpern, J., & Eracleous, M. 1999, *ApJ*, **523**, 197
- Kaper, L., Lamers, H. J. G. L. M., Ruymaekers, E., van den Heuvel, E. P. J., & Zuiderveld, E. J. 1995, *A&A*, **300**, 446
- Karasev, D. I., Lutovinov, A. A., & Burenin, R. A. 2010, *MNRAS*, **409**, L69
- Karasev, D. I., Tsygankov, S. S., & Lutovinov, A. A. 2008, *MNRAS*, **386**, L10
- Kaur, R., Casella, P., Linares, M., et al. 2010a, *ATel*, **3082**, 1
- Kaur, R., Paul, B., Kumar, B., & Sagar, R. 2008, *MNRAS*, **386**, 2253
- Kaur, R., Wijnands, R., Patruno, A., et al. 2009, *MNRAS*, **394**, 1597–604
- Kaur, R., Wijnands, R., Paul, B., Patruno, A., & Degenaar, N. 2010b, *MNRAS*, **402**, 2388
- Kendziorra, E., Kretschmar, P., Pan, H. C., et al. 1994, *A&A*, **291**, L31
- Kennea, J. A., Lien, A. Y., Krimm, H. A., Cenko, S. B., & Siegel, M. H. 2017, *ATel*, **10809**, 1
- Kim, V. Y., & Ikhsanov, N. R. 2017, *JPhCS*, **929**, 012005
- Kinugasa, K., Torii, K., Hashimoto, Y., et al. 1998, *ApJ*, **495**, 435
- Klus, H., Ho, W. C. G., Coe, M. J., Corbet, R. H. D., & Townsend, L. J. 2014, *MNRAS*, **437**, 3863
- Kouveliotou, C. 2002, Chandra Proposal, **04408146**
- Kretschmar, P., El Mellah, I., Martínez-Núñez, S., et al. 2021, *A&A*, **652**, A95
- Kretschmar, P., Fürst, F., Sidoli, L., et al. 2019, *NewAR*, **86**, 101546
- Kretschmar, P., Martínez-Núñez, S., Bozzo, E., et al. 2017, in IAU Symp. 329, The Lives and Death-Throes of Massive Stars, ed. J. J. Eldridge et al. (Cambridge: Cambridge Univ. Press), 355
- Kreykenbohm, I., Wilms, J., Coburn, W., et al. 2004, *A&A*, **427**, 975
- Krimm, H. A., Holland, S. T., Corbet, R. H. D., et al. 2013, *ApJS*, **209**, 14
- Krivonos, R. A., Sazonov, S. Y., Kuznetsova, E. A., et al. 2022, *MNRAS*, **510**, 4796
- Krivonos, R. A., Tsygankov, S. S., Lutovinov, A. A., et al. 2015, *ApJ*, **809**, 140
- Krtička, J. 2014, *A&A*, **564**, A70
- Kühnel, M., Müller, S., Kreykenbohm, I., et al. 2013, *A&A*, **555**, A95
- La Palombara, N., & Mereghetti, S. 2006, *A&A*, **455**, 283
- La Palombara, N., Sidoli, L., Esposito, P., Tiengo, A., & Mereghetti, S. 2009, *A&A*, **505**, 947
- La Palombara, N., Sidoli, L., Esposito, P., Tiengo, A., & Mereghetti, S. 2012, *A&A*, **539**, A82
- La Parola, V., Cusumano, G., Romano, P., et al. 2010, *MNRAS*, **405**, L66
- La Parola, V., Cusumano, G., Segreto, A., et al. 2013, *ApJL*, **775**, L24
- La Parola, V., Segreto, A., Cusumano, G., et al. 2014, *MNRAS*, **445**, L119
- Landi, R., Masetti, N., Capitanio, F., Fiocchi, M., & Bird, A. J. 2009, *ATel*, **2355**, 1
- Li, J., Wang, W., & Zhao, Y. 2012a, *MNRAS*, **423**, 2854
- Li, J., Zhang, S., Torres, D. F., et al. 2012b, *MNRAS*, **426**, L16
- Li, K. J., Zhang, J., & Feng, W. 2017, *MNRAS*, **472**, 289
- Lin, X. B., Church, M. J., Nagase, F., & Bafucińska-Church, M. 2002, *MNRAS*, **337**, 1245
- Lipunov, V. M. 1982, *SvA*, **26**, 537
- Lipunov, V. M. 1992, Astrophysics of Neutron Stars (Berlin: Springer)
- Liu, Q. Z., van Paradijs, J., & van den Heuvel, E. P. J. 2000, *A&AS*, **147**, 25
- Liu, Q. Z., van Paradijs, J., & van den Heuvel, E. P. J. 2006, *A&A*, **455**, 1165
- Lorenzo, J., Negueruela, I., Castro, N., et al. 2014, *A&A*, **562**, A18
- Lutovinov, A., Revnivtsev, M., Gilfanov, M., et al. 2005a, *A&A*, **444**, 821
- Lutovinov, A., Rodriguez, J., Revnivtsev, M., & Shtykovskiy, P. 2005b, *A&A*, **433**, L41
- Lutovinov, A. A., Buckley, D. A. H., Townsend, L. J., Tsygankov, S. S., & Kennea, J. 2016, *MNRAS*, **462**, 3823
- Lutovinov, A. A., Tsygankov, S. S., Karasev, D. I., Molkov, S. V., & Doroshenko, V. 2019, *MNRAS*, **485**, 770
- Lutovinov, A. A., Tsygankov, S. S., Postnov, K. A., et al. 2017, *MNRAS*, **466**, 593
- Lyne, A., & Graham-Smith, F. 2012, Pulsar Astronomy (Cambridge: Cambridge Univ. Press)
- Lyubimkov, L. S., Rostopchin, S. I., Roche, P., & Tarasov, A. E. 1997, *MNRAS*, **286**, 549
- Maccarone, T. J., Girard, T. M., & Casetti-Dinescu, D. I. 2014, *MNRAS*, **440**, 1626
- Maitra, C., Raichur, H., Pradhan, P., & Paul, B. 2017, *MNRAS*, **470**, 713
- Maíz Apellániz, J., Sota, A., Morrell, N. I., et al. 2013, in ASP Conf. Ser. 465, Four Decades of Research on Massive Stars, ed. L. Drissen et al. (San Francisco, CA: ASP), 484
- Makishima, K., Mihara, T., Ishida, M., et al. 1990, *ApJL*, **365**, L59

- Malacaria, C., Bhargava, Y., Coley, J. B., et al. 2022, *ApJ*, **927**, 194
- Malacaria, C., Jenke, P., Roberts, O. J., et al. 2020, *ApJ*, **896**, 90
- Marcu-Cheatham, D. M., Pottschmidt, K., Kühnel, M., et al. 2015, *ApJ*, **815**, 44
- Markwardt, C. B., Baumgartner, W. H., Skinner, G. K., & Corbet, R. H. D. 2010, ATel, **2564**, 1
- Marsden, D., Gruber, D. E., Heindl, W. A., Pelling, M. R., & Rothschild, R. E. 1998, *ApJL*, **502**, L129
- Marshall, N., & Ricketts, M. J. 1980, *MNRAS*, **193**, 7P
- Masetti, N., Mason, E., Morelli, L., et al. 2008, *A&A*, **482**, 113
- Masetti, N., Parisi, P., Palazzi, E., et al. 2009, *A&A*, **495**, 121
- Mason, A. B., Clark, J. S., Norton, A. J., Negueruela, I., & Roche, P. 2009, *A&A*, **505**, 281
- Mason, A. B., Norton, A. J., Clark, J. S., Negueruela, I., & Roche, P. 2010, *A&A*, **509**, A79
- McBride, V. A., Wilms, J., Coe, M. J., et al. 2006, *A&A*, **451**, 267
- McBride, V. A., Wilms, J., Kreykenbohm, I., et al. 2007, *A&A*, **470**, 1065
- McCollum, B., & Laine, S. 2019, ATel, **13211**, 1
- McKinney, W. 2010, in Proc. 9th Python in Science Conf., ed. S. van der Walt & J. Millman, 56
- Mereghetti, S., & La Palombara, N. 2009, *A&A*, **504**, 181
- Molkov, S., Lutovinov, A., Tsygankov, S., Mereminskiy, I., & Mushtukov, A. 2019, *ApJL*, **883**, L11
- Morel, T., & Grosdidier, Y. 2005, *MNRAS*, **356**, 665
- Motch, C., Haberl, F., Dennerl, K., Pakull, M., & Janot-Pacheco, E. 1997, *A&A*, **323**, 853
- Mukerjee, K., & Antia, H. M. 2021, *ApJ*, **920**, 139
- Mukerjee, K., Antia, H. M., & Katoch, T. 2020, *ApJ*, **897**, 73
- Müller, S., Kühnel, M., Caballero, I., et al. 2012, *A&A*, **546**, A125
- Mushtukov, A. A., Suleimanov, V. F., Tsygankov, S. S., & Poutanen, J. 2015, *MNRAS*, **454**, 2539
- Nabizadeh, A., Mönkkönen, J., Tsygankov, S. S., et al. 2019a, *A&A*, **629**, A101
- Nabizadeh, A., Tsygankov, S. S., Karasev, D. I., et al. 2019b, *A&A*, **622**, A198
- Nabizadeh, A., Tsygankov, S. S., Molkov, S. V., et al. 2022, *A&A*, **657**, A58
- Nagase, F. 1989, *PASJ*, **41**, 1
- Nagase, F., Dotani, T., Tanaka, Y., et al. 1991, *ApJL*, **375**, L49
- Naik, S., Maitra, C., Jaiswal, G. K., & Paul, B. 2013, *ApJ*, **764**, 158
- Negueruela, I. 1998, *A&A*, **338**, 505
- Negueruela, I., Casares, J., Verrecchia, F., et al. 2008, ATel, **1876**, 1
- Negueruela, I., Israel, G. L., Marco, A., Norton, A. J., & Speziali, R. 2003, *A&A*, **397**, 739
- Negueruela, I., & Okazaki, A. T. 2001, *A&A*, **369**, 108
- Negueruela, I., Roche, P., Fabregat, J., & Coe, M. J. 1999, *MNRAS*, **307**, 695
- Negueruela, I., & Schurch, M. P. E. 2007, *A&A*, **461**, 631
- Nespoli, E., Fabregat, J., & Mennickent, R. E. 2008, *A&A*, **486**, 911
- Nespoli, E., Fabregat, J., & Mennickent, R. E. 2010, *A&A*, **516**, A94
- Nespoli, E., & Reig, P. 2011, *A&A*, **526**, A7
- Nespoli, E., Reig, P., & Zezas, A. 2012, *A&A*, **547**, A103
- Neumann, M., Avakyan, A., Doroshenko, V., & Santangelo, A. 2023, arXiv, [2303.16137](#)
- Nikolov, Y. M., Zamanov, R. K., Stoyanov, K. A., & Martí, J. 2017, BlgAJ, **27**, 10
- Nowak, M. A., Paizis, A., Rodriguez, J., et al. 2012, *ApJ*, **757**, 143
- O'Connor, B., Göğüş, E., Huppenkothen, D., et al. 2022, *ApJ*, **927**, 139
- Oh, S., & Kroupa, P. 2016, *A&A*, **590**, A107
- Oja, T. 1991, *A&AS*, **89**, 415
- Orlandini, M., Frontera, F., Masetti, N., Sguera, V., & Sidoli, L. 2012, *ApJ*, **748**, 86
- Pacini, F. 1970, *Natur*, **226**, 622
- Pahari, M., & Pal, S. 2012, *MNRAS*, **423**, 3352
- Parkes, G. E., Murdin, P. G., & Mason, K. O. 1978, *MNRAS*, **184**, 73P
- Pearlman, A. B., Coley, J. B., Corbet, R. H. D., & Pottschmidt, K. 2019, *ApJ*, **873**, 86
- Piraino, S., Santangelo, A., Segreto, A., et al. 2000, *A&A*, **357**, 501
- Postnov, K. A., Mironov, A. I., Lutovinov, A. A., et al. 2015, *MNRAS*, **446**, 1013
- Pradhan, P., Maitra, C., Paul, B., & Paul, B. C. 2013, *MNRAS*, **436**, 945
- Pringle, J. E., & Rees, M. J. 1972, *A&A*, **21**, 1
- Puls, J., Vink, J. S., & Najarro, F. 2008, *A&ARv*, **16**, 209
- Quaintrell, H., Norton, A. J., Ash, T. D. C., et al. 2003, *A&A*, **401**, 313
- Raddi, R., Irrgang, A., Heber, U., Schneider, D., & Kreuzer, S. 2021, *A&A*, **645**, A108
- Rahoui, F., & Chaty, S. 2008, *A&A*, **492**, 163
- Rahoui, F., Chaty, S., Lagage, P. O., & Pantin, E. 2008, *A&A*, **484**, 801
- Raichurch, H., & Paul, B. 2010, *MNRAS*, **406**, 2663
- Raman, G., Varun, P. B., & Bhattacharya, D. 2021, *MNRAS*, **508**, 5578
- Ray, P. S., & Chakrabarty, D. 2002, *ApJ*, **581**, 1293
- Reed, B. C. 2003, *AJ*, **125**, 2531
- Reig, P., Belloni, T., Israel, G. L., et al. 2008, *A&A*, **485**, 797
- Reig, P., Blinov, D., Papadakis, I., Kyrafis, N., & Tassis, K. 2014a, *MNRAS*, **445**, 4235
- Reig, P., & Coe, M. J. 1999, *MNRAS*, **302**, 700
- Reig, P., Doroshenko, V., & Zezas, A. 2014b, *MNRAS*, **445**, 1314
- Reig, P., & Fabregat, J. 2015, *A&A*, **574**, A33
- Reig, P., & Fabregat, J. 2022, *A&A*, **667**, A18
- Reig, P., Fabregat, J., & Alfonso-Garzón, J. 2020, *A&A*, **640**, A35
- Reig, P., Fabregat, J., Coe, M. J., et al. 1997, *A&A*, **322**, 183
- Reig, P., Negueruela, I., Fabregat, J., et al. 2004, *A&A*, **421**, 673
- Reig, P., Negueruela, I., Fabregat, J., Chato, R., & Coe, M. J. 2005a, *A&A*, **440**, 1079
- Reig, P., Negueruela, I., Papamastorakis, G., Manousakis, A., & Kougentakis, T. 2005b, *A&A*, **440**, 637
- Reig, P., Nespoli, E., Fabregat, J., & Mennickent, R. E. 2011, *A&A*, **533**, A23
- Reig, P., & Roche, P. 1999, *MNRAS*, **306**, 100
- Reig, P., Roche, P., Fabregat, J., & Coe, M. J. 1996, in Roentgenstrahlung from the Universe, ed. H. U. Zimmermann, J. Trümper, & H. Yorke, 181
- Reig, P., & Zezas, A. 2014, *MNRAS*, **442**, 472
- Reig, P., & Zezas, A. 2018, *A&A*, **613**, A52
- Riquelme, M. S., Torrejón, J. M., & Negueruela, I. 2012, *A&A*, **539**, A114
- Rodes-Roca, J. J., Bernabeu, G., Magazzù, A., Torrejón, J. M., & Solano, E. 2018, *MNRAS*, **476**, 2110
- Rodes-Roca, J. J., Torrejón, J. M., Martínez-Núñez, S., Bernabéu, G., & Magazzù, A. 2013, *A&A*, **555**, A115
- Romanó, P., Bozzo, E., Mangano, V., et al. 2015, *A&A*, **576**, L4
- Romanó, P., Sidoli, L., Cusumano, G., et al. 2009, *ApJ*, **696**, 2068
- Rouco Escorial, A., van den Eijnden, J., & Wijnands, R. 2018, *A&A*, **620**, L13
- Roy, J., Agrawal, P. C., Singari, B., & Misra, R. 2020, *RAA*, **20**, 155
- Sadakane, K., Hirata, R., Jugaku, J., et al. 1985, *ApJ*, **288**, 284
- Şahiner, Ş., Inam, S. Ç., & Baykal, A. 2012, *MNRAS*, **421**, 2079
- Salganik, A., Tsygankov, S. S., Djupvik, A. A., et al. 2022, *MNRAS*, **509**, 5955
- Santangelo, A., del Sordo, S., Segreto, A., et al. 1998, *A&A*, **340**, L55
- Sarty, G. E., Kiss, L. L., Huziak, R., et al. 2009, *MNRAS*, **392**, 1242
- Sarty, G. E., Pilecki, B., Reichart, D. E., et al. 2011, *RAA*, **11**, 947
- Sato, N., Nagase, F., Kawai, N., et al. 1986, *ApJ*, **304**, 241
- Scott, D. M., Finger, M. H., Wilson, R. B., et al. 1997, *ApJ*, **488**, 831
- Segreto, A., La Parola, V., Cusumano, G., et al. 2013, *A&A*, **558**, A99
- Sguera, V., Drave, S. P., Sidoli, L., et al. 2013, *A&A*, **556**, A27
- Sguera, V., Hill, A. B., Bird, A. J., et al. 2007, *A&A*, **467**, 249
- Shakura, N. I. 1973, *SvA*, **16**, 756
- Shakura, N. I. 1975, *SvAL*, **1**, 223
- Shaw, S. E., Hill, A. B., Kuulkers, E., et al. 2009, *MNRAS*, **393**, 419
- Shirke, P., Bala, S., Roy, J., & Bhattacharya, D. 2021, *JApA*, **42**, 58
- Shtykovsky, A. E., Lutovinov, A. A., Tsygankov, S. S., & Molkov, S. V. 2019, *MNRAS*, **482**, L14
- Sidoli, L., Esposito, P., Motta, S. E., Israel, G. L., & Rodríguez Castillo, G. A. 2016, *MNRAS*, **460**, 3637
- Sidoli, L., Israel, G. L., Esposito, P., Rodríguez Castillo, G. A., & Postnov, K. 2017, *MNRAS*, **469**, 3056
- Sidoli, L., Mereghetti, S., Sguera, V., & Pizzolato, F. 2012, *MNRAS*, **420**, 554
- Sidoli, L., & Paizis, A. 2018, *MNRAS*, **481**, 2779
- Sidoli, L., Postnov, K., Tiengo, A., et al. 2020, *A&A*, **638**, A71
- Siuniaiev, R. A., & Shakura, N. I. 1977, *SvAL*, **3**, 114
- Staubert, R., Pottschmidt, K., Doroshenko, V., et al. 2011, *A&A*, **527**, A7
- Staubert, R., Trümper, J., Kendziorra, E., et al. 2019, *A&A*, **622**, A61
- Stevens, J. B., Reig, P., Coe, M. J., et al. 1997, *MNRAS*, **288**, 988
- Strader, J., Chomiuk, L., Swihart, S., & Aydi, E. 2019, ATel, **12554**, 1
- Sugizaki, M., Mitsuda, K., Kaneda, H., et al. 2001, *ApJS*, **134**, 77
- Sugizaki, M., Yamamoto, T., Miura, T., Nakajima, M., & Makishima, K. 2015, *PASJ*, **67**, 73
- Swank, J. H., & Markwardt, C. B. 2003, ATel, **128**, 1
- Taylor, M. B. 2005, in ASP Conf. Ser. 347, Astronomical Data Analysis Software and Systems XIV, ed. P. Shopbell, M. Britton, & R. Ebert (San Francisco, CA: ASP), 29
- Thompson, T., & Rothschild, R. 2008, *ApJ*, **691**, 1744
- Thompson, T. W. J., Tomsick, J. A., in 't Zand, J. J. M., Rothschild, R. E., & Walter, R. 2007, *ApJ*, **661**, 447
- Thompson, T. W. J., Tomsick, J. A., Rothschild, R. E., in 't Zand, J. J. M., & Walter, R. 2006, *ApJ*, **649**, 373
- Tobrej, M., Rai, B., Ghising, M., Tamang, R., & Paul, B. C. 2023, *MNRAS*, **518**, 4861

- Torii, K., Kinugasa, K., Katayama, K., et al. 1998, *ApJ*, **508**, 854
- Torrejón, J., Negueruela, I., Smith, D., & Harrison, T. 2010, *A&A*, **510**, 1
- Torrejón, J. M., Kreykenbohm, I., Orr, A., Titarchuk, L., & Negueruela, I. 2004, *A&A*, **423**, 301
- Torrejón, J. M., & Negueruela, I. 2007, ESA SP-622, The Obscured Universe. Proc. VI INTEGRAL Workshop (Noordwijk: ESA), **503**
- Torrejón, J. M., Negueruela, I., Smith, D. M., & Harrison, T. E. 2010, *A&A*, **510**, A61
- Tsygankov, S. S., Doroshenko, V., Mushtukov, A. A., Lutovinov, A. A., & Poutanen, J. 2019a, *A&A*, **621**, A134
- Tsygankov, S. S., Krivonos, R. A., & Lutovinov, A. A. 2012, *MNRAS*, **421**, 2407
- Tsygankov, S. S., Lutovinov, A. A., Krivonos, R. A., et al. 2016, *MNRAS*, **457**, 258
- Tsygankov, S. S., Lutovinov, A. A., Molkov, S. V., et al. 2021, *ApJ*, **909**, 154
- Tsygankov, S. S., Rouco Escorial, A., Suleimanov, V. F., et al. 2019b, *MNRAS*, **483**, L144
- Tutukov, A. V., & Cherepashchuk, A. M. 2020, *PhyU*, **63**, 209
- Uchida, N., Takahashi, H., Fukazawa, Y., & Makishima, K. 2021, *PASJ*, **73**, 1389
- UKIDSS Consortium 2012, yCat, **2316**, 0
- van den Heuvel, E. P. J. 2017, in Handbook of Supernovae, ed. A. W. Alsabi & P. Murdin (Cham: Springer), **1527**
- van Paradijs, J. 1995, in X-ray Binaries, ed. W. H. G. Lewin, J. van Paradijs, & E. P. J. van den Heuvel (Cambridge: Cambridge Univ. Press), **536**
- Wang, W. 2010, *A&A*, **516**, A15
- Wang, W. 2011, *MNRAS*, **413**, 1083
- Wang, W. 2014, *RAA*, **14**, 565
- Wen, L., Remillard, R. A., & Bradt, H. V. 2000, *ApJ*, **532**, 1119
- Wenger, M., Ochsenbein, F., Egret, D., et al. 2000, *A&AS*, **143**, 9
- Wilson, C. A., Finger, M. H., & Camero-Arranz, A. 2008, *ApJ*, **678**, 1263
- Wilson, C. A., Finger, M. H., Coe, M. J., & Negueruela, I. 2003, *ApJ*, **584**, 996
- Wilson, C. A., Finger, M. H., Göğüş, E., Woods, P. M., & Kouveliotou, C. 2002, *ApJ*, **565**, 1150
- Wilson, C. A., Finger, M. H., Harmon, B. A., et al. 1997, *ApJ*, **479**, 388
- Wilson, C. A., Finger, M. H., Harmon, B. A., Chakrabarty, D., & Strohmayer, T. 1998, *ApJ*, **499**, 820
- Wilson, C. A., Finger, M. H., & Scott, D. M. 1999, *ApJ*, **511**, 367
- Wilson-Hodge, C. A. 1999, PhD thesis, Univ. Alabama, Huntsville
- Wilson-Hodge, C. A., Malacaria, C., Jenke, P. A., et al. 2018, *ApJ*, **863**, 9
- Yamamoto, T., Sugizaki, M., Mihara, T., et al. 2011, *PASJ*, **63**, S751
- Yan, J., Zurita Heras, J. A., Chaty, S., Li, H., & Liu, Q. 2012, *ApJ*, **753**, 73
- Yungelson, L. R., Kuranov, A. G., & Postnov, K. A. 2019, *MNRAS*, **485**, 851
- Zacharias, N., Finch, C. T., Girard, T. M., et al. 2012, yCat, **1322**, 0
- Zhang, S., Qu, J.-L., Song, L.-M., & Torres, D. F. 2005, *ApJL*, **630**, L65
- Zhao, Y., Heinke, C. O., Tsygankov, S. S., et al. 2019, *MNRAS*, **488**, 4427
- Zurita Heras, J. A., & Chaty, S. 2008, *A&A*, **489**, 657
- Zurita Heras, J. A., De Cesare, G., Walter, R., et al. 2006, *A&A*, **448**, 261